Contributions to the FEL'95 Conference, August 20 - 26, 1995 in New York City, USA

September 1995, TESLA-FEL 95-04

Contents TESLA FEL Report 95-04

The Bunch Compression System at the TESLA Test Facility FEL

T. Limberg, H. Weise
DESY, Notkestraße 85, 22603 Hamburg, Germany

A. Molodozhentsev, V. Petrov
JINR, Dubna, Russia

Abstract

A SASE-FEL requires extremely high peak currents which cannot be achieved by electron guns. The bunch length therefore has to be reduced along the accelerating linac, the bunch has to be compressed. In the TTF-FEL this is done with the help of bending magnet chicanes in three stages. We present the lay-out of the scheme as well as first beam dynamics calculations.

PROOFS: T. Limberg

DESY/MPY

Notkestraße 85

22603 Hamburg

Germany

tel.: +49 40 8998 3998

fax: +49 40 8998 4305

e-mail: limberg@batman.desy.de

I. Introduction

Space charge effects prevent electron guns from producing bunches considerably shorter than 1mm while maintaining the brightness necessary for a SASE-FEL[1]. A bunch compression system is needed to compress the bunch down to its final length of less than 100 μm, thus providing the necessary high peak intensities at the undulator.

Figure 1 shows the principle of bunch compression in longitudinal phase space. The uncorrelated energy spread of the beam leaving the gun is around 25 keV, its length 2 mm. The SASE process requires less than 1000 keV energy spread at the undulator. The initial longitudinal emittance of around 50 mm·keV is already close to the finally tolerable emittance, so emittance blow up during compression has to be kept small.

In an ideal bunch compressor, a linear correlation between energy and longitudinal position is induced to the bunch for instance by passing a high gradient RF structure at the zero-crossing phase. Then follows a sequence of bending magnets where particles with different energies have different path lengths; mostly because they travel on circles with different radii through the bending magnets with dispersion. The dependence between path length and particle energy is therefore in very good approximation linear and with the right choice of parameters an ideal full compression as shown in Fig. 1 can be achieved. The final bunch length is basically determined by the ratio of initial to induced energy spread.

Compressing the bunch in the TTF-FEL will be done in stages to negotiate two effects limiting the achievable bunch length: On one hand, a long bunch traveling through the whole linac accumulates too much nonlinear although correlated energy spread from the cosine-like accelerating RF field. We looked into compressors with nonlinear dependence between path length and energy spread to compensate for that, but found that introducing these non-linearities gives rise to other non-linear terms like higher order dispersion which then dilute the emittance.

On the other hand, space charge effects scale with $1/\gamma^2$ and prevent bunch compression resulting in very short bunches if the energy is still too low. Also, longitudinal wake field effects get stronger if the bunches are shorter. The following chapter describes the resulting layout of the bunch compression system in the TTF-FEL.

II. Layout of the TTF-FEL Bunch Compression System

As shown in Figure 2, the bunch compression will be done in three stages. The first compressor might be considered part of the electron injector since it is located directly after the first 15 MeV acceleration section and compresses a 2 mm bunch down to a little below 1 mm.
In the next step, after the first RF module, the bunch is further compressed to 0.3 mm at an energy of 144 MeV and the third step reaches the final value of 0.05 mm.

A schematic drawing of bunch compressors two and three is shown in Fig. 3. The stage 1 compressor looks essentially the same but for being half as long. The bending magnets are rectangular magnets which do not have net focusing in the horizontal plane and therefore do not generate higher order dispersion that would increase transverse emittance. They do focus the beam vertically, the focal length being inversely proportional to the tangent of the entrance angle of the beam. For bending (and entrance) angles of more than 30 degrees additional quadrupoles have to be considered between the bending magnets to avoid too densely focused beams in the vertical plane which would cause emittance growth due to space charge effects. For the proposed bunch compression system however, deflection angles of up to 23 degrees are sufficient.

In Figure 4, the maximum horizontal dispersion and the resulting 'longitudinal dispersion' R56 are shown. The path length difference Δl of an off-energy particle is given by

$$\Delta l = -R56 * \Delta E.$$

The choice of the necessary tuning range for the longitudinal dispersion determines the range in deflection angle for the bending magnets and thus the width of bending magnet gaps and vacuum chamber. The aperture in the middle bends and the instrumentation section is given by the sum of the orbit displacement in the magnet due to orbit curvature, the difference in beam orbits due to different dispersion values plus the dispersion dominated beam size of 20 mm (4 sigma of a beam with 1% energy spread at 0.5 m dispersion).

We have designed a bending magnet which allows deflection angles between 17 and 23 degrees at both the 140 and the 500 MeV compressor, resulting in a comfortable R56 tuning range of 0.12–0.24 m. It is a C-type magnet with a gap width of 360 mm and a good field region of 210 mm (relative field strength deviation less than $2*10^{-3}$).

The optics through the compressor magnets is adjusted with the quadrupole triplets on both sides of the bending magnets. Their strengths are chosen to match the incoming optics parameters to the outgoing to make the compressor section transparent and keep it symmetric around the mid-plane. Fig. 5 shows horizontal and vertical beam sizes (normalized with respect to transverse emittance) and the dispersion function in the TTF-FEL from the source up to the third compressor stage.

III. Simulation Calculations

Bunch compression has been simulated in two different ways. A one-dimensional model including the nonlinear RF and longitudinal wake fields was used to do a first optimization of RF phases and the longitudinal dispersion R56 of the compressor sections. To study space charge effects and subsequently re-optimize the compression scheme, three-dimensional calculations using the code PARMELA were done. The dipoles were set to deflection angles of 18 degrees in compressor 2 and 20 degrees in compressor 3.

Calculations with a One-Dimensional Model:

In the one-dimensional model, it was assumed that the bunch leaves the injector with 0.8 mm bunch length and a random energy spread of 25 keV. Figure 6 shows the bunch in longitudinal phase space before and after compressor 2 at a beam energy of 145 MeV. Note that the bunch is not fully compressed to avoid problems with space charge effects. The bunch then passes through three RF modules, where it experiences the non-linear shape of the RF pulse as well as longitudinal wake fields. The phase of the bunch has to be optimized to achieve the best cancellation of both effects. Figure 7 shows the result of such an optimization: the bunch entering the final compression stage 3 has a nearly linear correlation between energy and longitudinal position over a wide range and can therefore be compressed down to 54 μm.

In the last part of the linac, where the bunch is accelerated to 1 GeV, its longitudinal distribution does not change anymore. Its energy spread, however, will be increased by RF non-linearities and wake fields. Here again the RF phase has to be adjusted to minimize growth in energy spread. As to be seen in figure 6.8, the bunch gains another 130 keV of energy spread on its way to the undulator.

3-Dimensional Calculations with PARMELA:

To evaluate space charge effects, the computer code PARMELA was used with a point-to-point algorithm to calculate space charge effects, since inside the compression sections the beam is not cylindrically symmetric. For these calculations all three bunch compressors were modeled with their optical elements. Figure 9 shows a PARMELA run without space charge. The RMS-value for bunch length is 0.075 mm but is dominated by the tails of the distribution. More than 70% of the charge is within a window of ±0.05 mm, which supplies the necessary peak current.

If space charge effects are included (Figure 10), the distribution broadens, the RMS-value is nearly unchanged, but the charge contained within ±0.05 mm drops to about 60%, which is still within specifications.

The energy spread in both calculations is of the order of 500 keV, but wake fields are not yet included in these calculations, so it is expected to be closer to 1 MeV like in the one-dimensional calculations.

IV. Conclusion and Outlook

We propose a bunch compression in three stages to avoid longitudinal emittance blow up due to space charge forces on one hand and nonlinear RF energy correlation on the other. We have found optical solutions, transverse and longitudinal, to fit the compressor sections into the TTF linac. A bending magnet has been designed which meets the space requirements and provides a comfortable range of deflection angles. The first simulation calculations show that although space charge forces already increase longitudinal emittance, we still meet the SASE specifications.

We still have to introduce wake fields into the tracking, although the one-dimensional model does not predict a dramatic increase in energy spread. Perhaps more important are the effects of possible coherent synchrotron radiation on the energy distribution in the electron bunch, which are just being analyzed[5].

V. References

[2] A VUV Free Electron Laser at the TESLA Test Facility at DESY, Conceptual Design Report, DESY Print TESLA-FEL 95-03 (1995)

[1] A. M. Kontradenko, E. L. Saldin: Part. Acc. Vol. 10, p. 207-216 (1980)

[4] A. Derbenev, E. L. Saldin: private communication

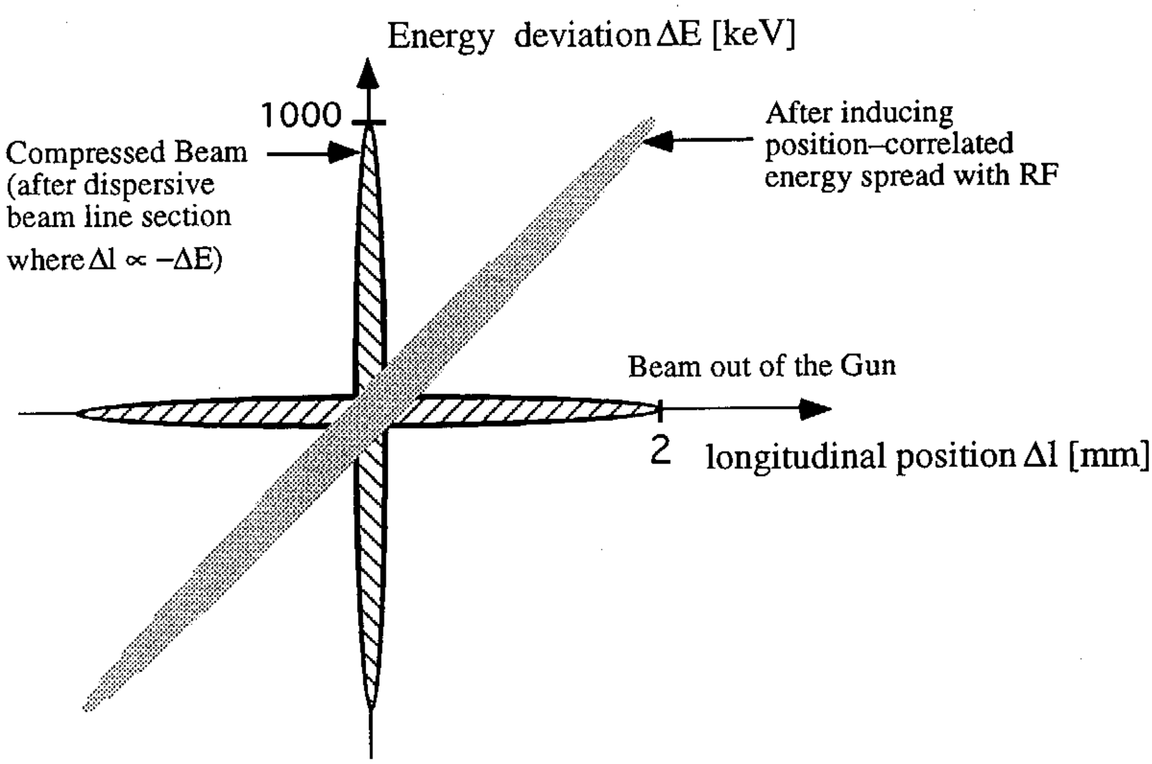

Fig. 1: Principle scheme of required bunch compression

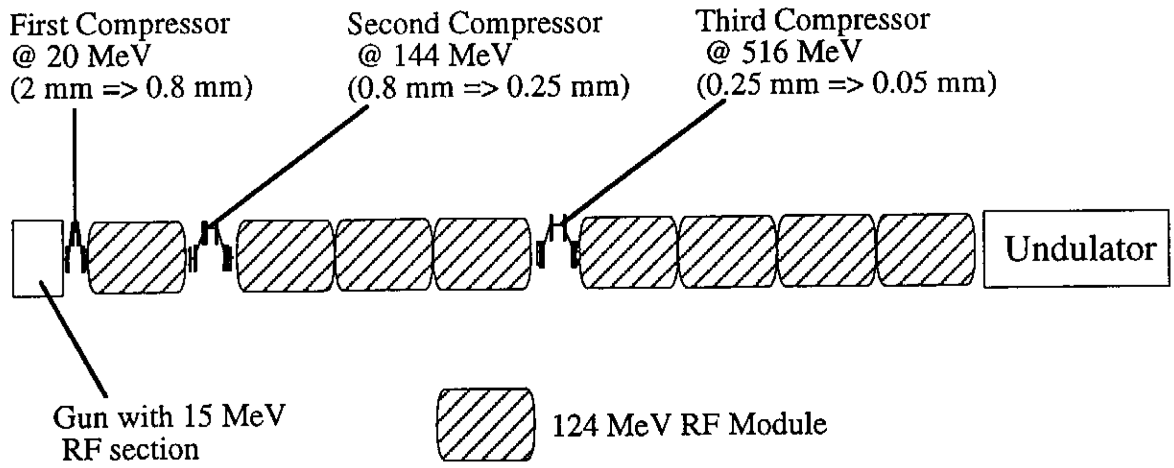

Fig. 2: Layout of the TTF-FEL Bunch Compression System

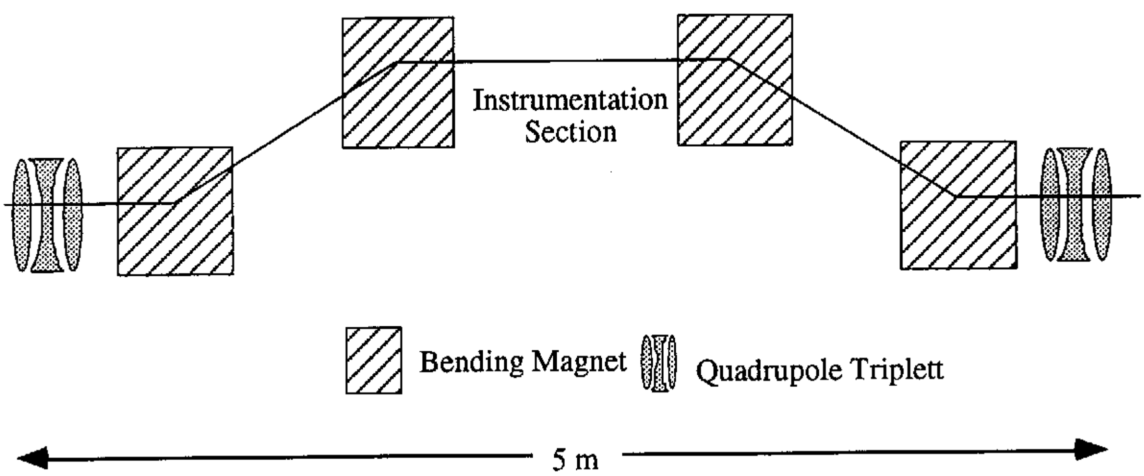

Fig. 3 : Lay Out of the Bunch Compressors at Stage 2 and 3

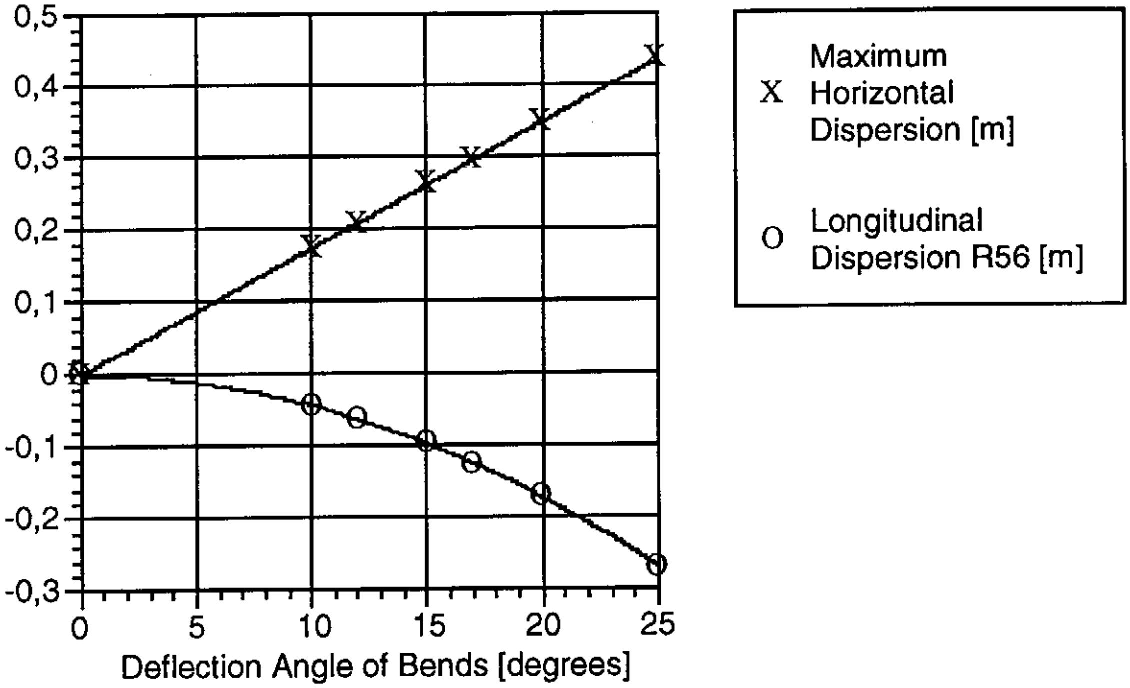

Fig. 4 Maximum Horizontal Dispersion and Longitudinal Dispersion R56 vs. Bending Magnet Deflection Angle in Bunch Compressors

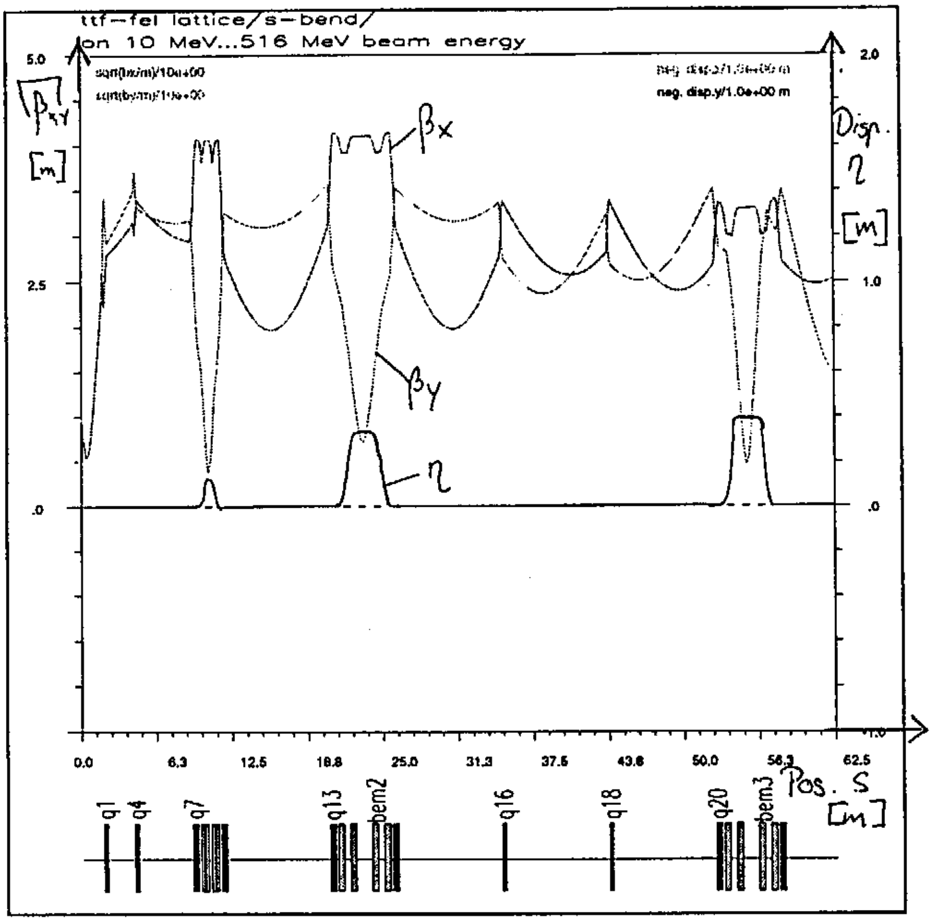

Fig. 5: Optical Functions in the TTF-Linac with Bunch compression 'on' from Source to 3rd Bunch Compressor

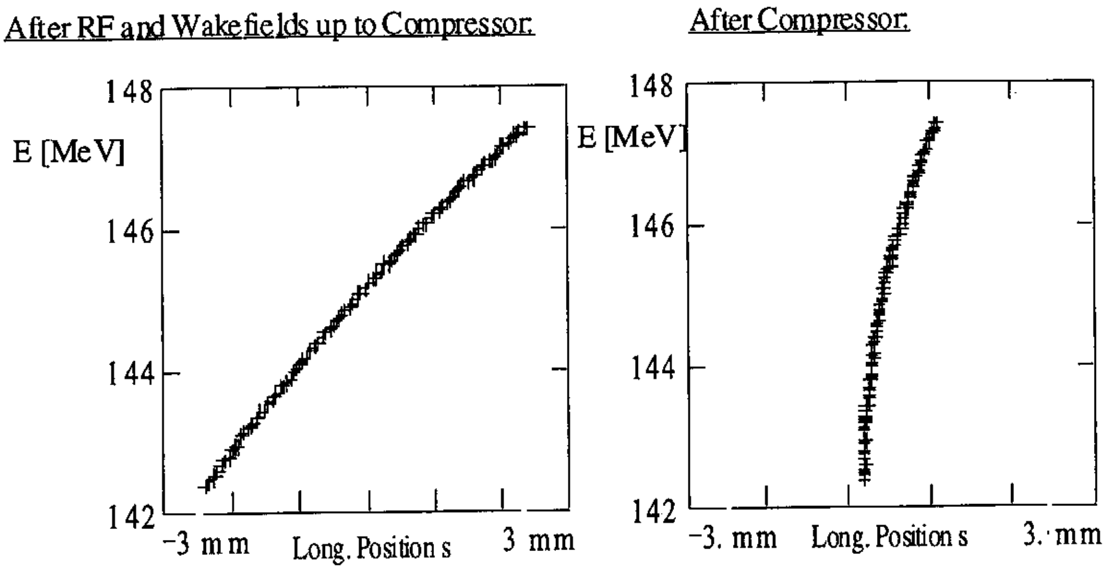

Fig. 6 : Longitudinal Phase Space before and after Bunch Compressors #2

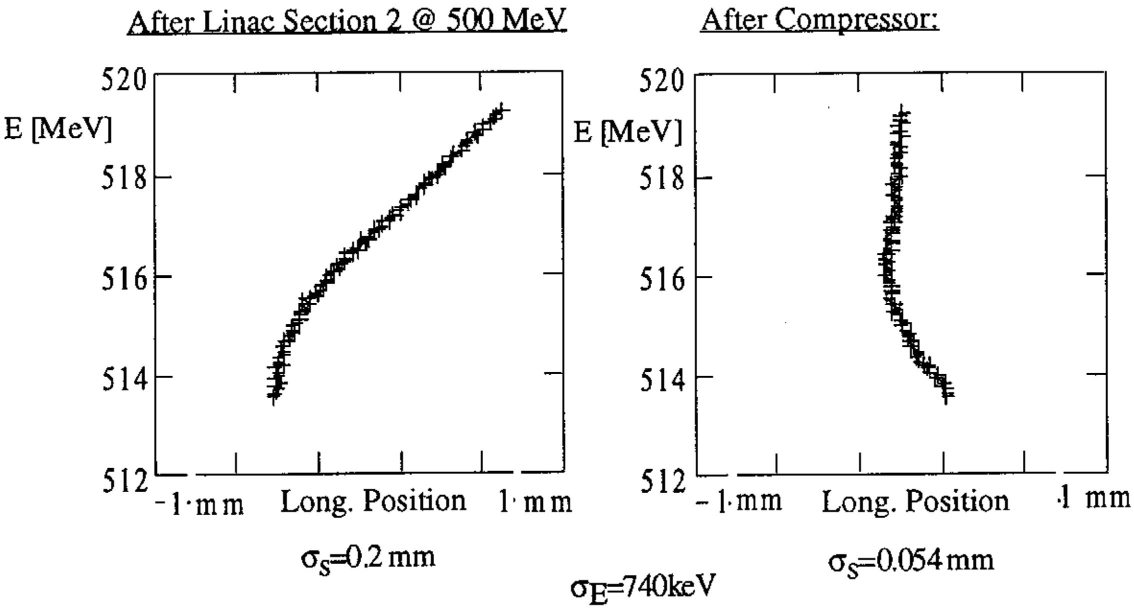

Fig. 7 : Longitudinal Phase Space before and after Bunch Compressors #3

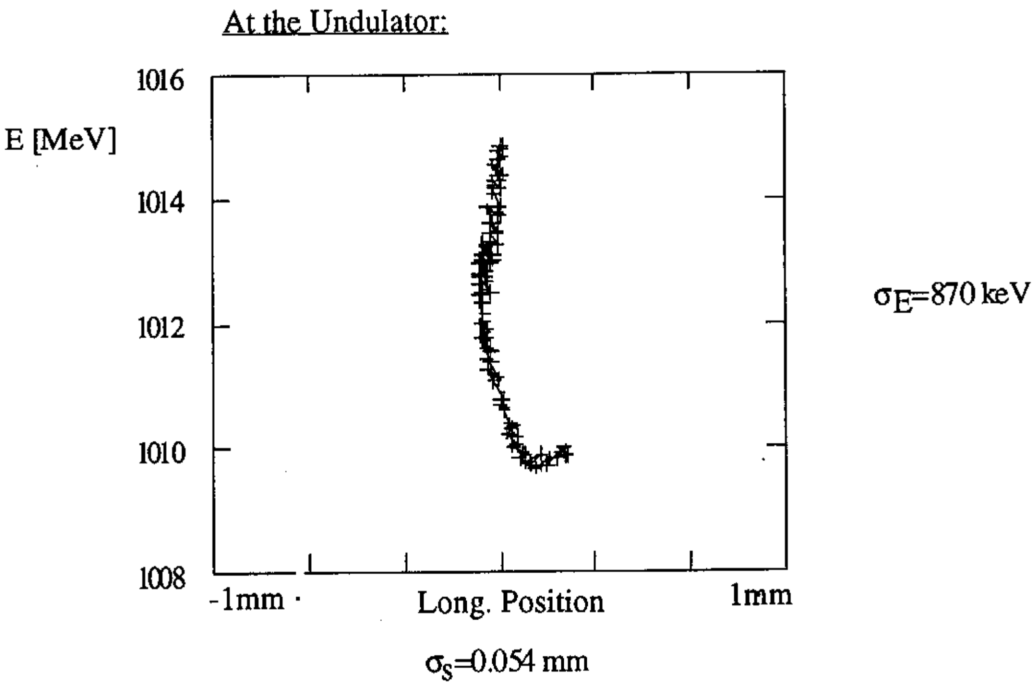

Fig. 8: Longitudinal Phase Space before Undulator

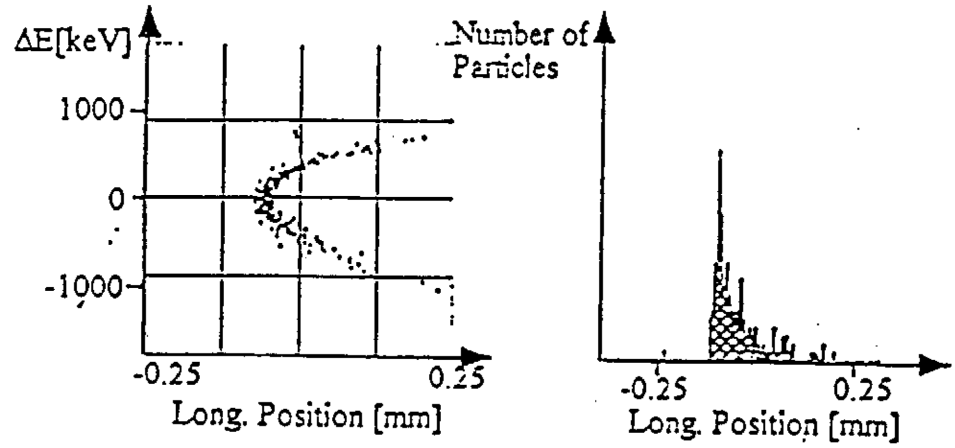

Fig. 9 Longitudinal Phase Space and Longitudinal Bunch Distribution after Bunch Compressor #3 without Space Charge Effects

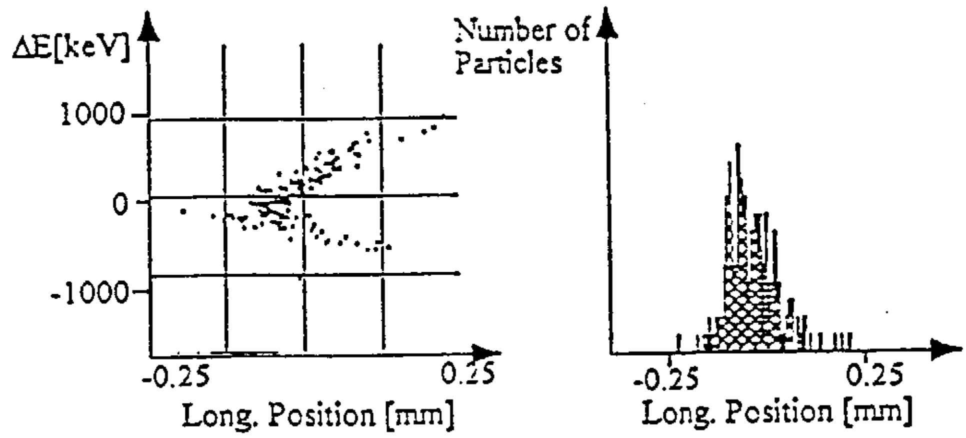

Fig. 10 Longitudinal Phase Space and Longitudinal Bunch Distribution after Bunch Compressors #3 with Space Charge Effects (bunch charge ≈1 nC)

DEPENDENCE OF THE VUV-FEL PERFORMANCE AT THE TESLA TEST FACILITY ON MAGNETIC FIELD ERRORS

B. Faatz[a], J. Pflüger[a] and P. Pierini[b]

[a]Hamburger Synchrotronstralungslabor, HASYLAB
at Deutsches Elektronen Synchrotron, DESY
Notkestr. 85, 22603 Hamburg, Germany

[b]INFN Milano-LASA, Via Cervi, 201, 20090 Segrate (MI), Italy

ABSTRACT

The VUV FEL, which is in its design stage at DESY, is a SASE device which is driven by a 1 GeV superconducting linac. In this paper, the performance of the 25 m long undulator, is studied. Results of simulations, including magnetic peak-field errors, are presented. Dependence of the performance on these errors is discussed.

1. Introduction

In designing a VUV-FEL, much effort is spent in reducing the electron beam energy spread and emittance. As one aims at shorter wavelengths, the phase space volume of the electron beam has to become smaller. For a SASE FEL, the undulator needs about 1000 periods. In this case the cumulative effect of magnetic field errors becomes another issue to take into account. During the past decade, both analytical and numerical studies have shown that two important parameters which determine the FEL performance are the phase of the electron with respect to the ponderomotive potential, as well as the beam wander, i.e., the deviation of the electron beam from the undulator axis [1-7].The first quantity determines the energy exchange between electrons and the field, the second determines the transverse overlap between electron beam as a whole and the radiation field.

The different error sources, such as variation in undulator wavenumber or random tilt of the poles, generating small undesirable magnetic field contributions in both transverse and longitudinal directions, are assumed to be either negligibly small, or are assumed to be well described by an effective random variation of the main peak field of the planar structure. The aim of this paper is to determine the influence of phase and overlap for the TTF-FEL parameters on the gain as well as to establish some general idea within what distance the electron beam has to remain from the optical axis, including the motion due to the FODO-lattice used to keep the beam confined within the specified radius of 57 μm. The design of the undulator with a superimposed FODO-lattice is studied in separate papers [8-9].

This paper is organized as follows. In section 2, some comments will be made on the influence of the error in magnetic peak field. The next section results of simulations for different error distributions are shown. In the last section the results are discussed and first estimations on tolerances are given.

2. Influence of magnetic field errors

From FEL physics, it is well known that two important quantities determine to large extent the FEL performance. One is the resonance condition, i.e., the phase of the electrons with respect to the ponderomotive potential, the second is the overlap between electron beam and field. The ponderomotive phase is approximated by

$$\psi \approx \psi_0 + \left(k_u - \frac{k_s}{2\gamma_0^2}\right) z - \frac{k_s}{2\gamma_0^2 k_u}\Delta\psi$$

$$\text{with } \Delta\psi(z) = k_u \int_0^z (\gamma_0\beta_x)^2 \, dz' , \qquad (1)$$

where k_u and k_s are the undulator and radiation wavenumber, respectively, γ_0 and β_x are the energy and transverse electron velocity normalized to the speed of light. Using $<\psi'>= 0$ to determine the resonant wavelength results in the following resonance condition

$$\lambda_s = \frac{\lambda_u}{2\gamma_0^2}\left(1 + \frac{<\Delta\psi>}{\pi N_u}\right) . \qquad (2)$$

Table 1: *Parameters of the TTF VUV-FEL*

Electron beam	
Energy	1 GeV
Peak current	2500 A
Normalized rms emittance	2π mm mrad
rms energy spread	0.1 %
External β-function	3 m
rms beam size in the undulator	57 μm
Undulator	
Type	Planar
Period	27.3 mm
Peak magnetic field	0.497 T
Magnetic gap	12 mm
Undulator module length	4.4 m
Effective undulator length	25 m
FODO-period	1.2 m
Quadrupole strength	4 T/m
Radiation	
Wavelength	6.4 nm

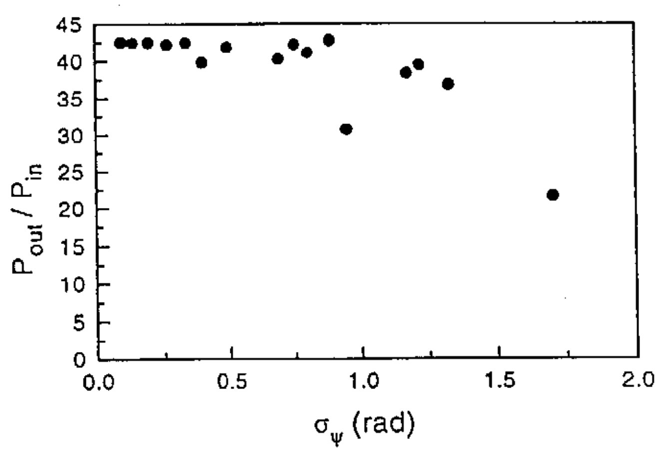

Figure 1: Normalized power versus rms phase-shake in case of an undulator field error per period after the first undulator module. Calculations have been performed in the one-dimensional limit, i.e., without FODO-lattice. Parameters as in Table 1.

With the resonant wavelength given by Eq. (2), we are now ready to calculate the phase shake. Its rms value is defined as the phase at the magnetic poles including errors minus the phase in case of ideal magnetic field squared and summed over all poles (see for example Ref. 5). With the definition of phase as given by Eq. (1), the ideal ψ is zero on the poles. Thus, the rms phase shake is

$$\sigma_\psi = \sqrt{\frac{1}{2N_u}\sum_{n=1}^{2N_u}\psi_n^2}\,, \tag{3}$$

where ψ_n is the phase evaluated on the poles. Poles are labeled by their appropriate number up to $2N_u$, with N_u the number of undulator periods.
In case of a non-ideal undulator, the derivative of β_x depends on the error of the n-th pole. Because the integral up to the n-th pole does not vanish, β_x depends all previous magnetic peak-field errors. Therefore, the electron beam trajectory may substantially deviate from the optical axis. Similar to the phase-shake, we also define

$$\sigma_x = \sqrt{\frac{1}{2N_u}\sum_{n=1}^{2N_u}x_n^2}\,, \tag{4}$$

where x_n is the second field integral evaluated on the magnetic poles, i.e., $x(z) = \int \beta_x(z')dz'$.
In order to describe a realistic undulator, one has to take into account the possibility to 'tune' the matching sections that set the first and second field integral equal to zero. A cos-field is assumed with constant peak field in case of an ideal unulator. Matching is achieved by starting and ending with quarter-periods instead of half. In all calculations it is assumed that the field amplitude of these two poles are adjusted such that first and second field integrals over the whole undulator field are equal to zero. The FODO-lattice is not taken into account in these adjustments.

3. Results of simulations

In this section, the model is applied to the TTF VUV-FEL (see Table 1 for details). Simulations have been performed with TDA3D [10-11].

Results given in Figs. 1 and 2 are obtained without FODO-lattice. The emittance is taken equal to zero. All other parameter are as in Table 1. In order to distinguish between phase shake, σ_ψ, and electron beam wander, σ_x, the normalized power ($P_{\rm out}/P_{\rm in}$) shown in Fig. 1 is obtained by using an error per undulator period instead of an error per half-period. Thus, the field integral per period is always zero and, consequently, the electron beam remains on axis. Of the two phenomena studied in this paper, only phase-shake can become large in this case. In order to get an rms phase-shake of the order of 1 radian for an undulator module of 4.4 m, as shown in Fig. 1, the field-amplitude error had to be increased to as much as 4 %. As can be seen, up to 0.5 rad, there is only a few percent decrease in power.

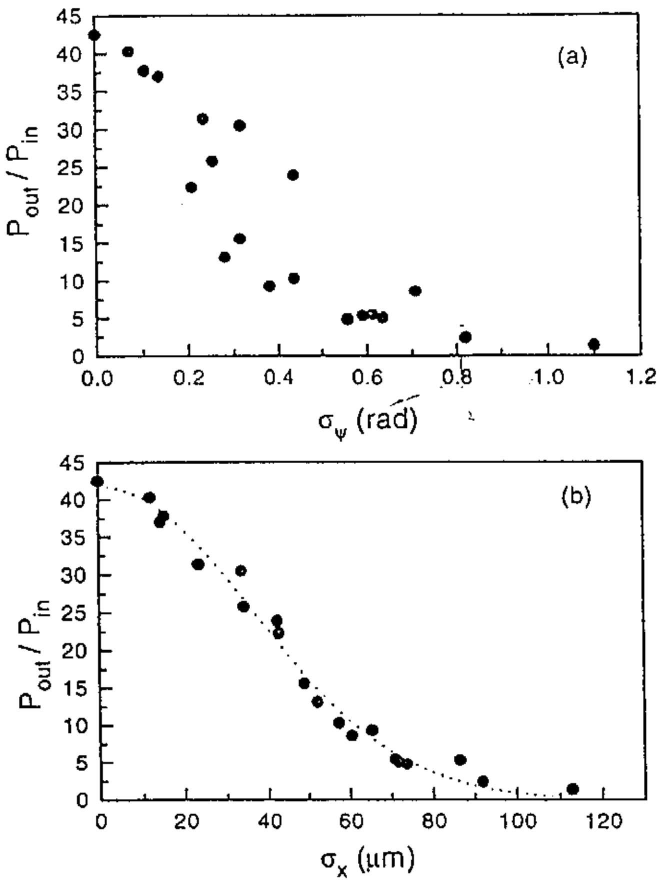

Figure 2: Normalized power versus rms phase-shake (a) and versus electron beam wander (b) in case of an undulator field error per half-period after the first undulator module. All remaining parameters as in Fig. 1.

In Fig. 2, errors are choosen per half period. Therefore, the electron beam can wander off-axis in this case. In all calculations, the rms field-amplitude error is 0.5 %, which is believed to be feasable. Fig. 2a shows again the normalized power versus rms phase shake. As can be seen, the power reduction is much larger than in the case with an error per period. The scatter of the points is much larger than in Fig. 1. In Fig. 2b, the nomalized power versus beam wander is shown. The dotted line is a Gaussian fit. As can be seen, the phase shake is not the principle parameter which determines the FEL performance in this case. It is dominated by the wander of the beam (see for example Ref. 4).

In calculations so far, the FODO-lattice was not taken into account. In case of an ideal undulator, i.e., without any errors, now including a FODO-lattice, the influence of electron beam mismatch is studied first. By giving the beam an initial transverse offset, it performes an oscillation throughout the whole undulator, thus reducing the overlap between electron beam and radiation field.

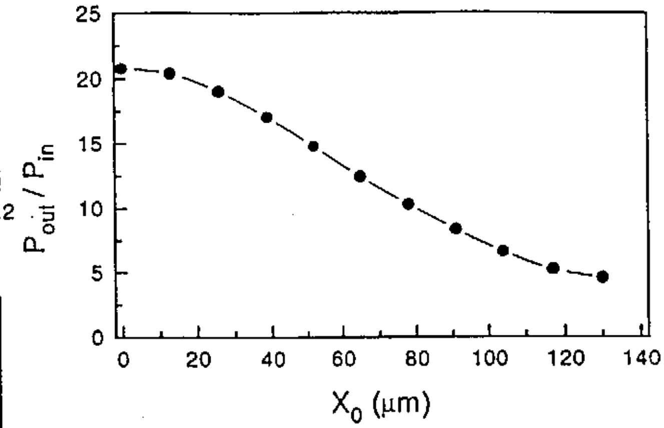

Figure 3: Normalized power versus initial beam offset. No undulator errors are included. Period of the FODO-lattice is 1.2 m.

In Fig. 3, the normalized power at the exit of one undulator module is shown for different values of the initial offset. Note that the normalized power in this case does not exceed 21, compared to 42 in the previous figures. This power reduction is caused by the non-zero emittance and focussing of the electron beam. The figure shows that the power reduction due to an initial offset can be approximated by $\exp(-X_0^2/2\sigma_b^2)$, where σ_b is the electron beam radius.

In Fig. 4, the performance of the FEL is shown including magnetic field errors and the FODO-lattice. It has been assumed the the focusing structure is ideal. Errors in this structure will be studied in a future paper. As can be seen, the results are similar to those obtained without focusing. The case without errors gives a normalized power of approximately 21, as in Fig. 3. With a σ_x of 10 μm, the reduction 10 %. We would like to stress that the value for σ_x has been calculated with Eq. (4), using the on-axis magnetic field, which is equivalent to neglecting the FODO-lattice. It does give, however, the deviation with respect to the ideal undulator.

In the TTF-FEL, we aim for four steering stations per module. This should result in an overlap which is large enough not to have a large gain reduction. According to Ref. 4, assuming a gain length of approximately 1.4 m (or 50 periods), a peak field error of 0.5 % and steering stations every 1.1 m, we find $W = 0.08$, and a gain reduction of less than 2 % (see Eq. (7.32) in Ref. 4).

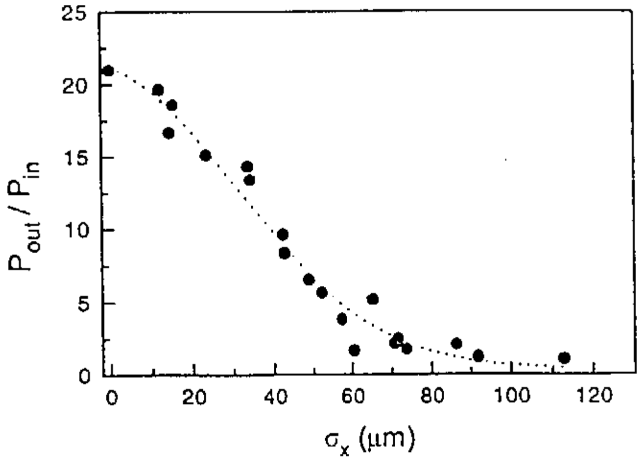

Figure 4: Normalized power versus electron beam wander in case of an undulator field error per half-period after the first undulator module including the FODO-lattice with a period of 1.2 m. All remaining parameters as in Fig. 1.

4. Discussion and conclusions

In case of the TTF-FEL, the dominant effect of magnetic field errors is the wander of the electron beam. Phase-shake with a perfectly aligned electron beam only gives a minor reduction in gain by a few percent per undulator module, whereas beam wander for the same rms-field error can give a gain-reduction by as much as an order of magnitude, if no additional steering is provided within the module.
Calculations including the FODO-lattice show that oscillations may not exceed 10 μm of maximum excursion (about $0.2\sigma_b$), giving a gain reduction of 10 %. With the 4 planned steering stations per module, the gain reduction is no more than a few percent.
We would like to stress that in the results presented in this paper, only the first undulator section has been taken into account. If the electron beam is perfectly matched at any section entrance, these results also hold for the five remaining ones, because the errors in the different sections ar independent. The main difference between the first and all remaining sections is, however, that the beam is not prebunched in these calculations. In order to calculate all remaining sections, we intend to modify TDA3D such that it can describe the modular setup of the TTF-FEL. To our understanding, however, the first undulator section will be the most crucial one, because the radiation field has to startup from noise.

Acknowledgement

We would like to thank Yu.M. Nikitina, H.D. Nuhn, C. Pellegrini, J. Roßbach, E.L. Saldin, E.A. Schneidmiller and M.V. Yurkov, for their interest in our work and the discussions we have had.

References

1. Brian M. Kincaid, J. Opt. Soc. Am. B **2** (1985) 1294.
2. H.D. Shay and E.T. Scharlemann, Nucl. Instr. Meth. **A272** (1988) 601.
3. John Vetrovec, IEEE J. Quant. Electron. **QE 27** (1991) 2673.
4. L.H. Yu, S. Krinsky, R.L. Gluckstern and J.B.J. Zeijts, Phys. Rev. A **45** (1992) 1163.
5. Richard P. Walker, Interference Effects in Undulator and Wiggler Radiation Sources Sincrotrone Trieste ST/M-93/3 (1993).
6. H.P. Freund and R.H. Jackson, Nucl. Instr. Meth. **A331** (1993) 461.
7. A. Friedman, S. Krinsky and L.H. Yu, IEEE J. Quant. Electron. **QE 30** (1994) 1295.
8. Yu.M. Nikitina and J. Pflüger, Two novel undulator schemes with quadrupolar focusing for the VUV-FEL at the TESLA Test Facility, presented at this conference.
9. J. Pflüger and Yu.M. Nikitina, Undulator schemes with the focusing properties for the VUV-FEL at the TTF, to be published.
10. T.-M. Tran and J.S. Wurtele, Comp. Phys. Commun. **54** (1989) 263.
11. P. Jha and J.S. Wurtele, Nucl. Instr. and Meth., **A331** (1993) 477.

Two novel undulator schemes with quadrupolar focusing for the VUV-FEL at the TESLA Test Facility

Yu.M. Nikitina*, J. Pflüger

Hamburger Synchrotronstrahlungslabor HASYLAB
at Deutsches Elektronen-Synchrotron DESY
Notkestr. 85, 22603 Hamburg, Germany
*) *Permanent address: Department of Mathematical Physics,*
Tomsk Polytechnical University , 634004 Tomsk, Russia

Abstract

At DESY in Hamburg a Free Electron Laser for the VUV spectral range at 6.4 nm using Self Amplified Spontaneous Emission is under construction. It will use the electron beam of the TESLA Test Facility. One of the main components is an undulator of 30 m length. In order to keep the electron beamsize small over the full undulator length an alternating quadrupole field has to be superimposed. In this paper two novel undulator schemes with these properties are proposed. The 3D-code MAFIA is used to calculate the magnetic properties. The results are presented and discussed.

PROOFS: J.Pflüger c.o.DESY, HASYLAB, Notkestr.85, 22603 Hamburg, Germany

Preprint submitted to Elsevier Science *8 September 1995*

Introduction

At DESY it has been decided to build a Free Electron Laser in the VUV spectral range (VUV-FEL) based on the principle of Self Amplified Spontaneous Emission (SASE) [1]. It will make use of the electron beam of the TESLA Test Facility (TTF), a linear accelerator which is already under construction [2]. The TTF will provide a very low normalized emittance ($\leq 2\pi mm \cdot mrad$), an ultra-short bunch length ($50\mu m$) and a peak current of about 2500 A. These properties will make the TTF an excellent driver for an FEL. At a nominal energy of 1 GeV, it will operate at a wavelength of 6.4 nm. In contrast to FEL's using optical cavities, a SASE FEL needs a very long undulator of a total length of about $30m$. Furthermore the undulator needs a superimposed quadrupolar field with an alternating gradient to produce a FODO lattice, which is used to keep the beamsize consistantly small over the whole undulator length.

There have been two different undulator schemes reported in literature which have focusing properties. One uses canted poles [3–5], the other makes use of an additional attachment of magnets to provide these properties [6,7]. The undulator structure, which is needed for a VUV-FEL at the TTF differs from other devices with similiar properties build so far in three aspects. First, a quadrupole lattice consisting of focusing, non-focusing and defocusing sections is needed to keep the beamsize at a constant low value over the whole length. Second, high gradients of up to 20 T/m are needed. Third, the undulator for the VUV-FEL will have a total length of about 30 meter. The requirements for the quality of the magnetic field will be high and need a precise magnetic characterization.

As a consequence, a magnetic assembly is desired which

1.) allows for a superimposed alternating gradient (FODO lattice)
2.) provides a sufficiently high gradient
3.) allows easy access to the field region for magnetic measurements and for the insertion of vacuum chambers.

In this report we propose two novel hybrid permanent magnet (PM) arrays, which have these properties. Both are planar and allow for completely free access to the field region.

A detailed study and comparison of these structures using the 3-D code MAFIA is presented. Only strong focusing as generated by quadrupolar fields is considered. Natural focusing as is present in any periodic field is neglected. The study is not a final design study. Its intention is to work out the potential of these structures for the undulator for the VUV-FEL.

The basic magnet design is based on Halbach's hybrid configuration [8]. The design parameters for this investigation were chosen to have the photon energy of the first harmonic at 192 eV at an electron energy of 1 GeV [1]. The magnetic design gap was conservatively assumed to be 12 mm. The period length was chosen to 27.3 mm. The peak field is about 0.5 T. The exact results may vary slightly for the different magnetic configurations investigated throughout this article.

Magnetic fields and gradients

In the iron free region, inside the gap an undulator field with a superimposed quadrupole field can be derived from a scalar potential of the form:

$$\chi = -\frac{B_{max}}{\kappa} \sinh \kappa y \sin \kappa z - Qxy \tag{1}$$

Here B_{max} is the peak field, Q the gradient, $\kappa = 2\pi/\lambda_0$ where λ_0 is the period length. The coordinate system is illustrated in Fig.1.

The magnetic field distribution is therefore given by:

$$\begin{aligned} B_x &= Qy \\ B_y &= B_{max} \cosh \kappa y \sin \kappa z + Qx \\ B_z &= B_{max} \sinh \kappa y \cos \kappa z \end{aligned} \tag{2}$$

The gradient may be obtained by:

$$\frac{\partial B_x}{\partial y} = \frac{\partial B_y}{\partial x} = Q \tag{3}$$

The field distributions, which can be generated by discrete permanent magnet arrays may differ considerably from the ideal ones given by eqs.(2). First, besides the pure quadrupole term Q, higher multipoles, such as octupoles *etc.*, may be present, especially when well away from the symmetry axis. Second, the gradient needs not to be constant along the electron beam direction. However, it will have the periodicity of the period length. It is therefore very useful to distinguish between the local, z-dependent gradient given by $Q = \partial B_y/\partial x$ and a gradient Q_{ave} averaged over an undulator period, which is defined as:

$$Q_{ave}(x,y) = \frac{1}{\lambda_u} \int_z^{z+\lambda_u} \frac{\partial B_y(x,y,z')}{\partial x} dz' = \frac{1}{\lambda_u} \frac{\partial}{\partial x} \int_z^{z+\lambda_u} B_y(x,y,z') dz' \tag{4}$$

where the integral in the second equation is the first field integral.

Four Magnets Focusing Undulator (4MFU)

Fig.1 shows the first proposal using four additional magnets per half-period. The magnets providing the undulator field (magnetized along z) have been recessed by 6 mm so that there is now space for the focusing magnets which are polarized parallel and anti-parallel along the y-direction as can be seen in Fig.1. This configuration is a modified adaptation from Tatchyn's proposal for generating quadrupolar fields with PM arrays [9]. The gap in this configuration is completely free. The achievable gradients depend on the height of the focusing magnets and their separation distance. The gradient becomes independent of the horizontal width of the focussing magnets if the width is choosen large enough. Fig.2 shows the tuning curve for the average gradient if the separation distance is changed. Gradients up to about 25 T/m can be obtained. To be on the safe side and to have some tunability to both sides a separation distance of 5.5 mm was taken with a corresponding gradient of 20 T/m. Fig.3 shows the transverse gradient along z at different x-values. It varies periodically along the electron beam axis with twice the frequency of the fundamental. It is smallest at the indicated pole positions. The RMS beamsize of the TTF is only 0.05 mm. At this x-value the gradient variation corresponds to a variation of the field amplitude with twice the frequency of the fundamental of $8.4 \cdot 10^{-4}$ T which is 0.17% of the peak amplitude. A preliminary list of design parameters can be found in Table 1.

Side Magnets Focusing Undulator (SMFU)

Fig.4 shows the other alternative using side magnets which extend over several poles. The magnets are brought close to the beam by choosing the width of the poles as small as possible (10 mm). The focusing magnets are embedded in the main magnets which produce the undulator field.

Fig.5 shows the average gradient as a function of the separation distance of the side magnets which cannot be smaller than 10 mm. The maximum average gradient is about 22 T/m. Finally, the variation of the mean gradient is shown in Fig.6. It is very x-dependent. However, extrapolation to the RMS beam-size of 0.05 mm shows variational amplitude of $5.4 \cdot 10^{-4}$ T corresponding to 0.11% of the peak amplitude. Table 1 summarizes the design parameters of the SMFU.

Summary and discussions

Two novel PM based hybrid structures with a periodic plus a quadrupole field have been proposed. Their inherent advantages are:

- They are completely planar. There is free access from the side for magnetic measurements and the insertion of a vacuum chamber.
- Field gradients larger than 20 T/m can be obtained for the parameters of the VUV-FEL at the TTF.
- Fine tuning by adjusting the focusing magnets is possible in both cases.
- The peak field in both proposals is independent of the focusing strength thus allowing for focusing, zero gradient and defocusing sections within an undulator without affecting the peak field.

A possible drawback of the SMFU may be its small pole width of only 10 mm as compared to the 12 mm wide gap. On the other hand, the beam of the TTF is very small and exact alignment of the focusing structure is required in any case in order to have the beam on the quadrupolar axis. The periodic variation of the field gradient along the z-axis might induce some effect which has to be investigated.

The work presented in this paper is part of a detailed analysis of a variety of PM structures with quadrupolar focusing. To some extent, the periodic variation of the gradient seems to be an characteristic for all structures, which has been investigated [10]. The influence of the periodic perturbations on the FEL performance will be the subject of another publication. First results indicate that the influence of the gradient variation can be neglected [11].

Acknowledgment

One of the authors (Y.M.N.) would like to thank HASYLAB for the hospitality during her stay in Hamburg and the DAAD for the financial support of this work.

References

[1] "A VUV Free Electron Laser at the TESLA Test Facility at DESY. Conceptual Design Report", DESY, Hamburg, June, 1995

[2] "TESLA Test Facility Linac - Design report", DESY, Hamburg, March, 1995

[3] K.E. Robinson, D.C. Quimby, J.M. Slater, IEEE Journal of Quantum Electronics Vol. QE-23, 9 (1987) 1497

[4] D.C. Quimby, S.C. Gottschalk, F.E. James, K.E. Robinson, J.M. Slater, A.S. Valla, Nucl.Instr. and Meth. A285 (1989) 281

[5] R. Schlüter in: Proceedings of the 16th FEL Conference August 21-26, 1994, Stanford, USA, Nucl. Instr. and Meth. A358 (1995) 44

[6] A.A. Varfolomeev, A.H. Hairetdinov Nucl.Instr. and Meth. A 341 (1994) 462

[7] A.A. Varfolomeev, V.V. Gubankov, A.H. Heiretdinov, S.N. Ivanchenkov, A.S. Khlebnikov, N.S. Osmanov, S.V. Tolmachev in: Proceedings of the 16th FEL Conference August 21-26, 1994, Stanford, USA, Nucl. Inst. and Meth. A358 (1995) 70

[8] K. Halbach, Journal de Physique, C1, suppl.2, (1983) C1-211

[9] R.Tatchyn, Nucl.Instr. and Meth. A341 (1994) 449

[10] J. Pflüger, Yu.M.Nikitina, in preparation

[11] Yu.M.Nikitina, J.Pflüger, E.Schneidmiller, in preparation

Figure captions

Figure 1. 3-D perspective view of 1 1/2 periods of the 4MFU hybrid undulator.

Figure 2. The dependence of the average gradient on the separation distance between the focusing magnets.

Figure 3. The variation of the gradient along the undulator axis for different values of x. Arrows indicate the location of the poles.

Figure 4. 3-D perspective view of 1 1/2 periods of the SMFU hybrid undulator.

Figure 5. The dependence of the average gradient on the separation distance between the focusing magnets.

Figure 6. The variation of the gradient along the undulator axis for different values of x. Arrows indicate the location of the poles.

Table 1		
PARAMETERS FOR	4MFU	SMFU
Period length	27.3 mm	27.3 mm
Peak field	0.5 T	0.5 T
Pole gap	12 mm	12 mm
Pole overhang	0.5 mm	0.5 mm
Focusing magnet separation	5.5 mm	12 mm
Magnet	70×50×10 mm	40×50×10 mm
Pole	50×40×3.65 mm	10×40×3.65 mm
Focusing magnet	15×6×10 mm	15×10× length of quad.
Gradient	20 T/m	20 T/m

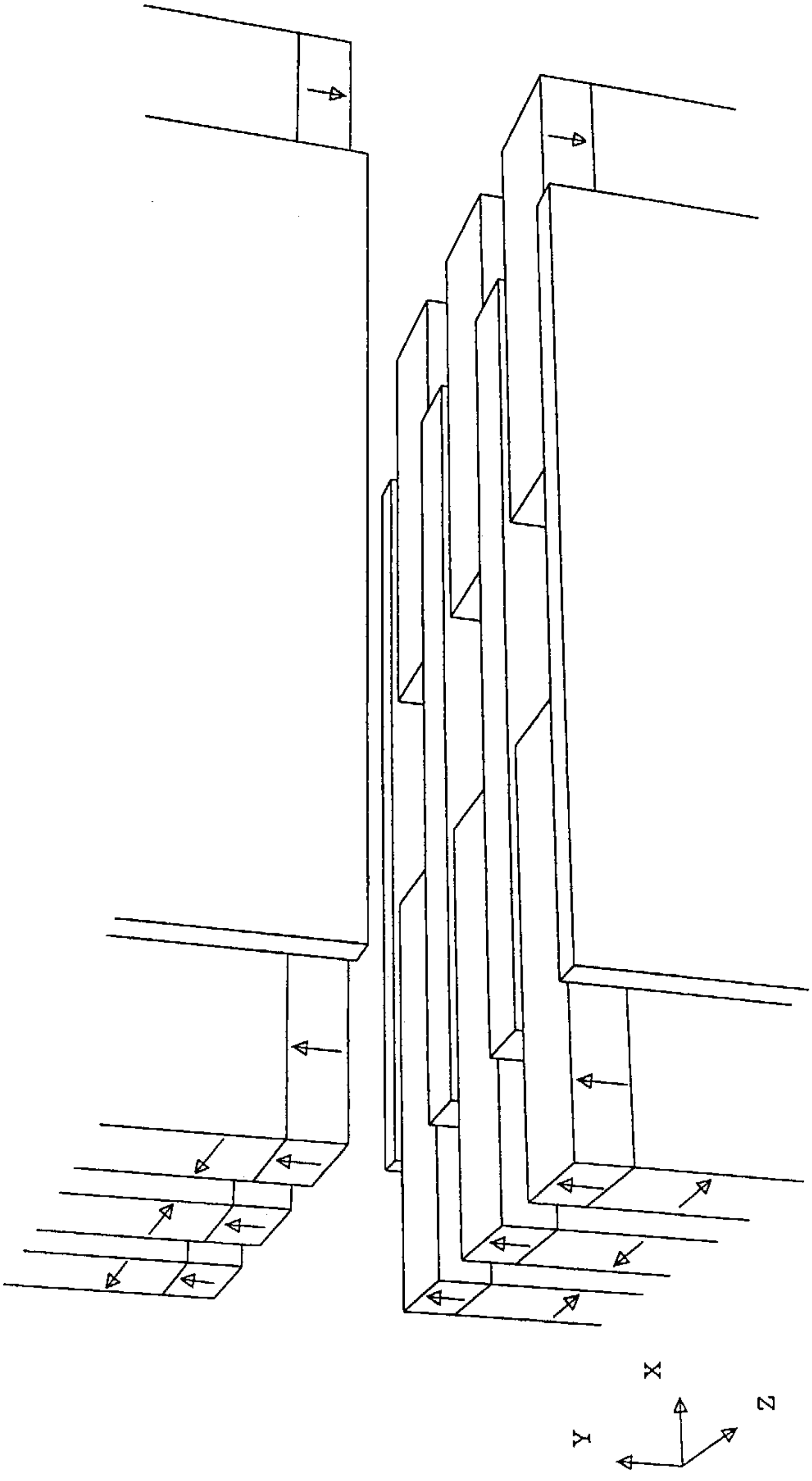
X
Y
Z

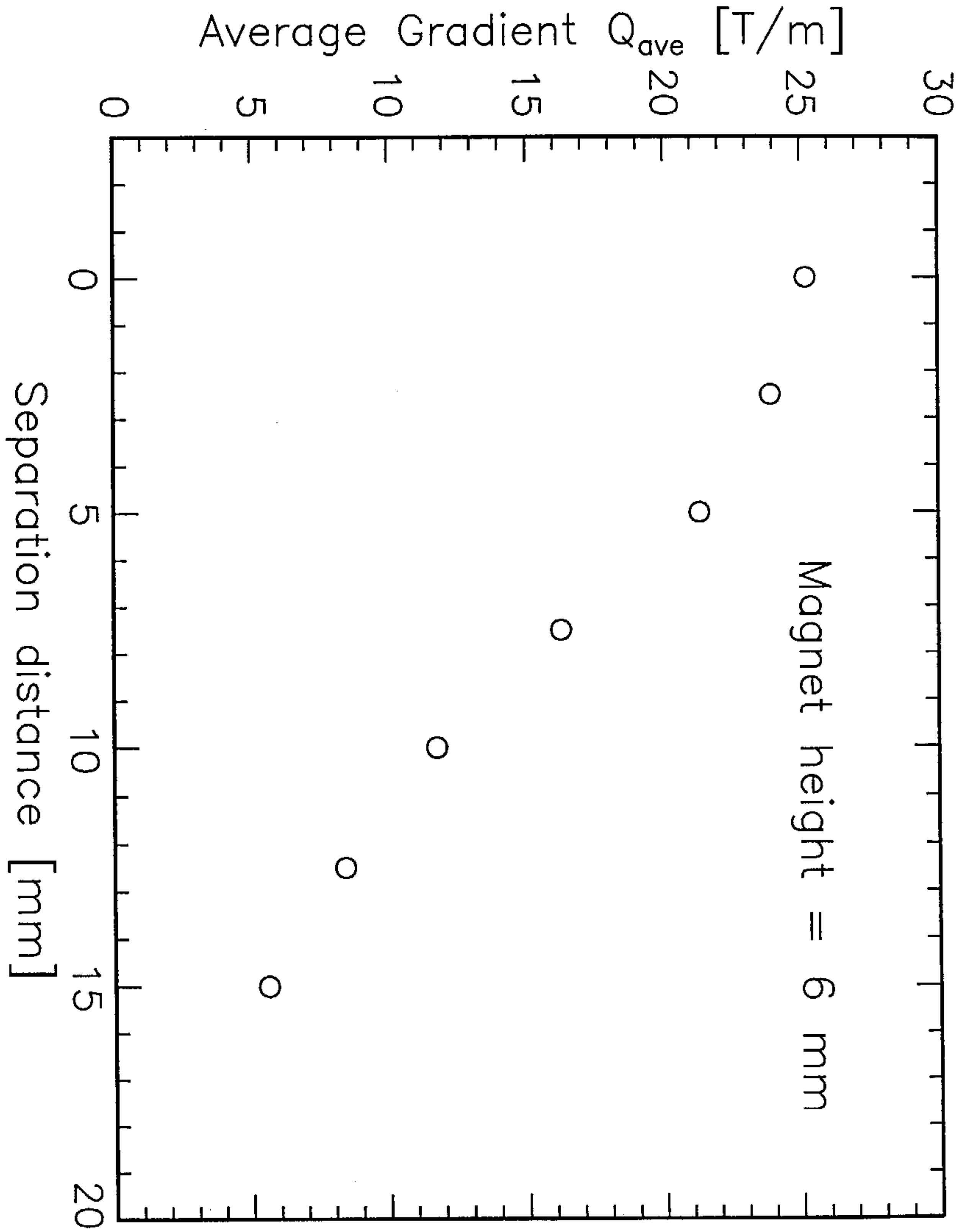
Average Gradient Q_{ave} [T/m]
0
5
10
15
20
25
30
Separation distance [mm]
0
5
10
15
20
Magnet height = 6 mm

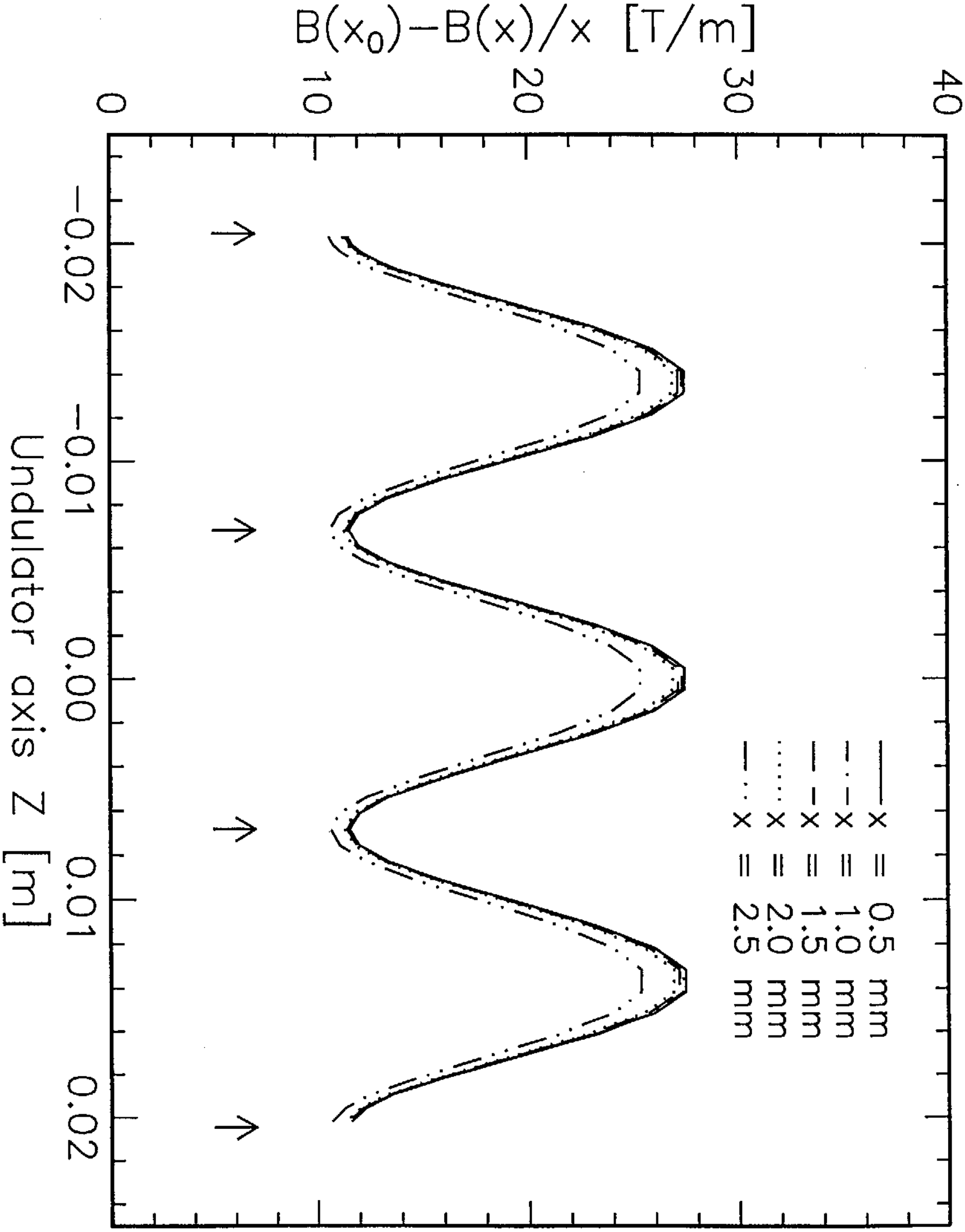
B(x₀)−B(x)/x [T/m]
0
10
20
30
40
−0.02
−0.01
0.00
0.01
0.02
Undulator axis Z [m]
x = 0.5 mm
x = 1.0 mm
x = 1.5 mm
x = 2.0 mm
x = 2.5 mm

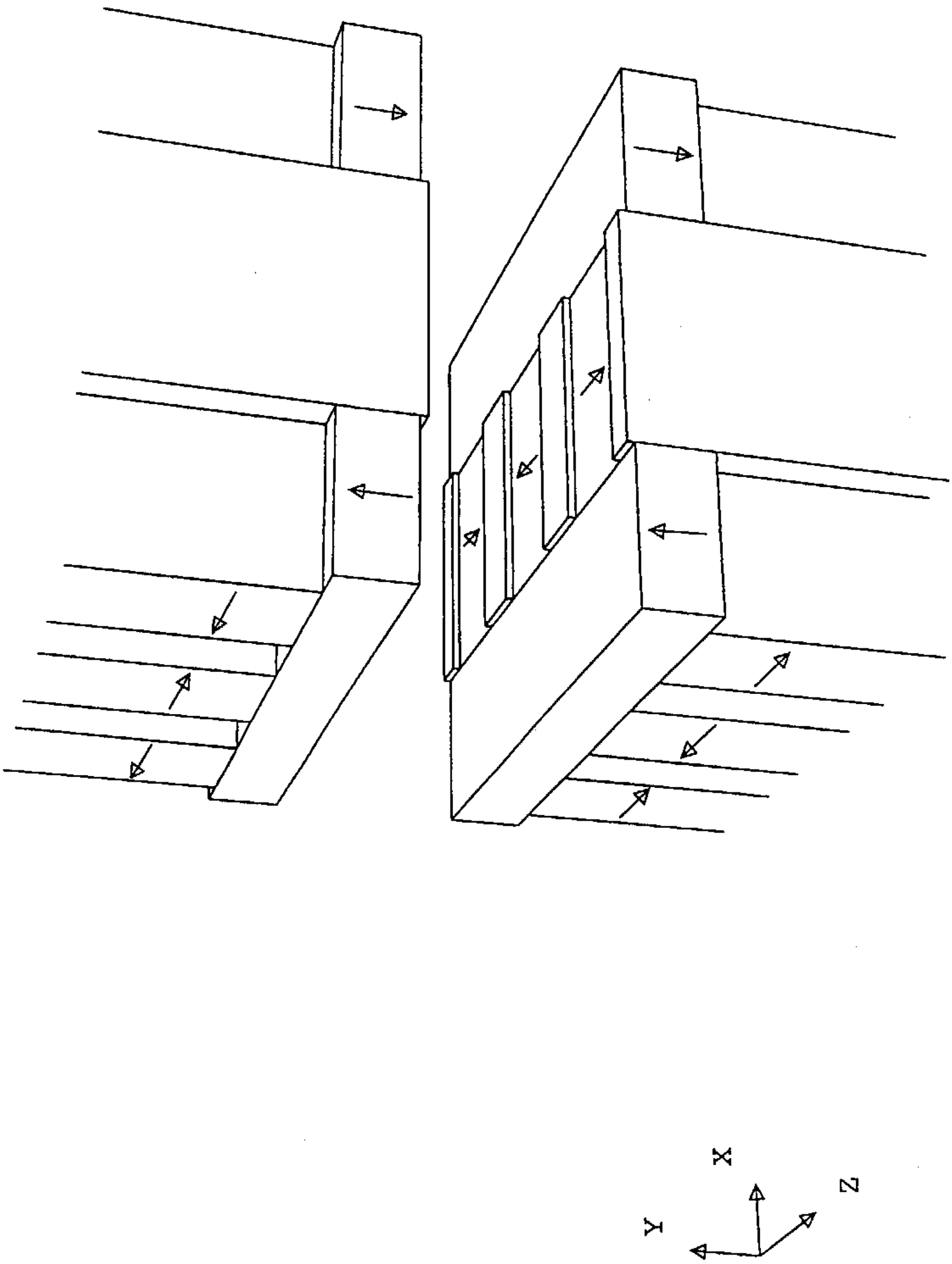
X
Y
Z

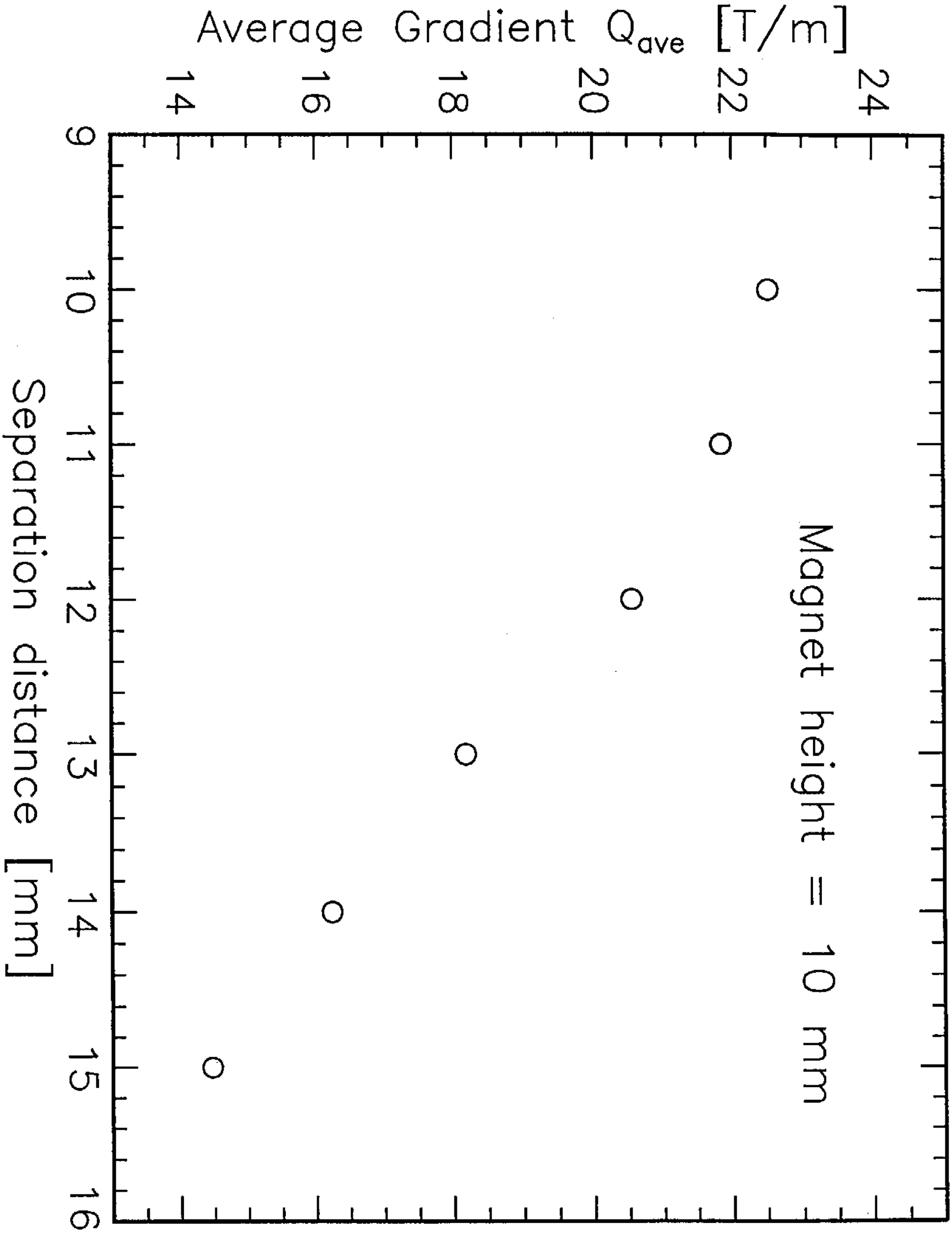
Average Gradient Qave [T/m]
14
16
18
20
22
24
9
10
11
12
13
14
15
16
Separation distance [mm]
Magnet height = 10 mm

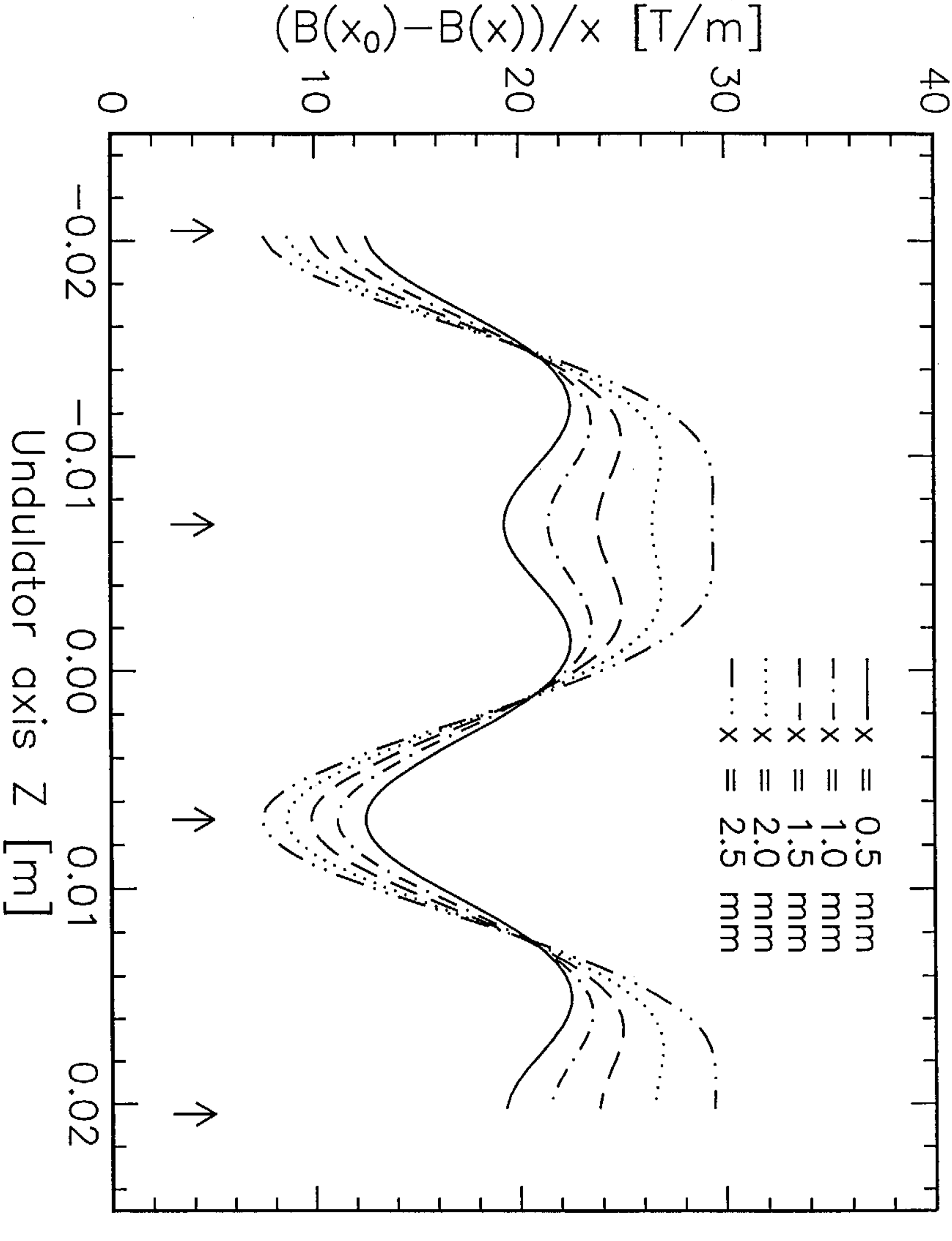

$(B(x_0)-B(x))/x$ [T/m]
Undulator axis Z [m]
x = 0.5 mm
x = 1.0 mm
x = 1.5 mm
x = 2.0 mm
x = 2.5 mm
0
10
20
30
40
-0.02
-0.01
0.00
0.01
0.02

Parameter study of the VUV FEL at the TESLA Test Facility

W. Brefeld[a], B. Faatz[a], Yu.M. Nikitina[a] [1], J. Pflüger[a], P. Pierini[b], J. Roßbach[a], E.L. Saldin[c], E.A. Schneidmiller[c], M.V. Yurkov[d]

[a] *Deutsches Elektronen Synchrotron, DESY, Notkestrasse 85, 22603 Hamburg, Germany*

[b] *INFN Milano - LASA, Via Cervi, 201, 20090 Segrate (MI), Italy*

[c] *Automatic Systems Corporation, Samara, Russia*

[d] *Joint Institute for Nuclear Research, Dubna, Russia*

Abstract

We present a short description of the theoretical and numerical activity for the design of the VUV FEL proposed at DESY. The FEL will be a 6 nm SASE device driven by a 1 GeV beam from the superconducting rf accelerator which is under development by the international TESLA collaboration.

1 Introduction

R&D on future generation linear colliders promises to give in the nearest future high-energy, low-emittance and monochromatic electron beams which could be used for a wide range of applications. One of them, which is under study at DESY, is to use the electron beam of the Tesla Test Facility (TTF) superconducting linear accelerator as a driving beam for a Self Amplified Spontaneous Emission (SASE) FEL operating at a 6.4 nm wavelength [1–3]. The obvious advantage of a SASE FEL compared to a seeded FEL amplifier is the fact that it does not need a master oscillator, unavailable at these short wavelengths [4].

One of the problems in designing a SASE FEL is to determine the characteristics of the generated radiation. In a traditional FEL amplifier scheme, the radiation generated by a narrow bandwidth master oscillator, which can be controlled both in amplitude and frequency, is amplified. Under these initial conditions the field amplitude of the radiation generated in the undulator does not depend on time, but only

[1] Permanent address: Department of Mathematical Physics, Tomsk Polytechnical University, 634004 Tomsk, Russia

Preprint submitted to Elsevier Science *15 August 1995*

on the spatial coordinates. This was the main factor which has allowed development of a wide range of reliable theoretical approaches, e.g. steady-state models, for calculation of characteristics of an amplifier [5] - [13]. Contrary to the traditional FEL amplifier, in a SASE FEL fluctuations of the beam current density play the role of input signal. These fluctuations vary in time and the associated spectrum is "white". To describe such a situation and to address the problem of longitudinal coherence, a time-dependent theory of the FEL amplifier should be used. For the analysis of transverse coherence, the time-dependent model should be extended to a full three dimensional model.

Nevertheless, the theoretical approach developed for the description of traditional FEL amplifiers can be used to find some characteristics of the SASE FEL. First of all, such an approach allows one to calculate the main characteristics of the radiation modes. This is a consequence of the fact that the "effective" power of the input signal is rather small with respect to the saturation power. As a result, only the mode having the largest growth rate survives. The characteristics of this mode do not depend on the nature of the input signal used, and are determined by the amplifier parameters. Therefore, with the aid of the results obtained with steady-state theory it is possible to calculate the gain and radial field distribution. Calculations of the frequency characteristic of the FEL amplifier allow to estimate the maximal bandwidth of the SASE FEL. Calculation of the amplitude characteristic of the FEL makes it possible to estimate the influence of the fluctuations of the input onto output amplitude. Using estimations of the "effective" power of shot noise we can calculate an approximate saturation length of the device.

Special attention is payed to the undulator of the VUV-FEL. In order to achieve saturation in a single pass, an undulator of a total length of 30 m is required. To keep the beamsize small over the whole undulator length, additional focusing has to be provided. A very suitable arrangement for that is a quadrupole lattice consisting of focusing and defocusing sections (FODO-lattice). The plan is to realize it by the incorporation of alternating field gradients into a hybrid permanent magnet (PM) structure. Structures, which fulfill these requirements, as well as investigation of the influence of field errors, are described elsewhere [1,14,16].

We have performed an optimization of the FEL amplifier characteristic using different 2D/3D simulation codes. Furthermore, we began to employ existent codes to calculate time-dependent effects [17].

2 Numerical simulation codes

The SASE FEL characteristics have been calculated with different 2D/3D steady-state simulation codes.

2.1 NUTMEG and GINGER

The codes NUTMEG and GINGER consider 2D axisymmetric radiation field and take into account the 3D electron motion in an undulator, allowing the use of an external focusing field [8]. Diffraction and guiding, effects of finite beam emittance and undulator errors, are included in the model. NUTMEG is a steady state simulation code. It provides a possibility to calculate higher harmonics of the emitted radiation and simulate multiple undulator schemes. The code GINGER extends the model to include time-dependent effects, and properly takes into account the longitudinal structure of electron beam and radiation field, and the slippage between pulses. GINGER can also model the shot noise startup by means of an incoherent random noise over the initial electron pulse without needing any equivalent input signal to start the SASE process, and can give information on the temporal and spectral characteristics of the emitted radiation.

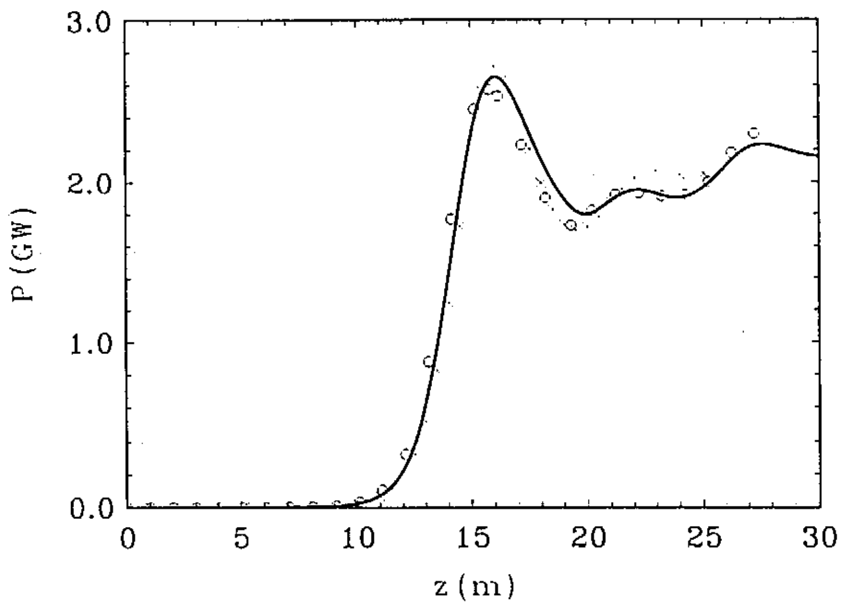

Fig. 1. Dependency of the FEL output power on the undulator length calculated with diferent simulation codes. Solid curve – FS2RN code, crosses – NUTMEG code and circles – TDA3D code.

2.2 TDA3D

The code TDA3D solves the electron and wave equations in the paraxial, single frequency approximation [9]. The wave equation is expanded into azimuthal modes to take into account non-axisymmetric effects in the interaction process. Equations are averaged over an undulator period, with the exception of the error term in the undulator field. An external FODO lattice is taken into account without a smooth approximation.

2.3 FS2R

The program package FS2R has been designed for calculations of an FEL amplifier with an axisymmetric electron beam. It covers all the aspects of the calculations of FEL amplifiers with an axisymmetric electron beam and consists of three codes [13], namely FS2RD (analysis of the eigenvalue problem), FS2RL (analysis of the initial-value problem) and FS2RN (nonlinear simulation code). Codes FS2RD and FS2RL are essentially based on the use of analytical techniques and FS2RN makes use of Green's function methods for the calculation of the radiation field.

In Fig.1 we show the dependence on the undulator length of the output radiation power of the FEL amplifier. It is seen that the codes give similar results.

3 Calculations of the SASE FEL performance

The region of parameters has been studied analytically [18,19] and with numerical simulation codes [1,19]. Taking into account technical limitations, we have chosen the parameters of the SASE FEL to be as close as possible to optimal ones (see Table 1) [1]. For the chosen parameters, the influence of the space charge field is negligible. A general analysis of the TTF FEL, presented in refs. [1,19], includes the study of undulator design, the influence of the imperfections of the undulator magnetic field and the beam quality on the FEL amplifier operation, time-dependent effects, etc. In this section we illustrate with numerical examples some characteristics of the SASE FEL. In the calculations we have simulated the initial conditions for the input signal as a gaussian laser beam. The value of "effective" power of the input signal due to fluctuations of the beam current density has been chosen in accordance with refs. [19,20].

3.1 Influence of the emittance

Fig.2 shows the influence of the emittance on the operation of the FEL. In the figure we plot the saturated power and saturation length at the peak FEL gain, using the parameters listed in Table 1. We can see from the figure that, in order to reach saturation within the currently envisaged undulator length of 25 to 30 m, the beam emittance at the undulator should not exceed 3-4π mm mrad. For bigger values of the emittance the FEL operation is not destroyed, but would require much longer

Table 1
General parameters of SASE FEL at DESY

Electron beam	
Energy	1000 MeV
Peak current	2500 A
Normalized rms emittance (Gaussian)	2π mm mrad
rms energy spread (Gaussian)	0.1 %
rms bunch length	50 μm
Bunch separation	111 ns
Number of bunches per train	7200
Repetition rate	10 Hz
External β-function	3 m
rms transverse beam size in the undulator	57μm
Undulator	
Type	Planar
Period	2.73 cm
Peak magnetic field	0.4972 T
Magnetic gap	1.2 cm
Effective undulator length	25 m
Radiation	
Wavelength	6.42 nm
Bandwidth	0.5 %
rms spot size at the undulator exit	130 μm
rms angular divergence	15 μrad
Peak power	5.5 GW
Average power	130 W
# of photons per electron bunch	7×10^{13}
Peak flux of photons	2×10^{26} photons/s
Average flux of photons	6×10^{18} photons/s
Peak brilliance	7×10^{29} photons/s/mm^2/mrad^2/0.1 %
Average brilliance	2×10^{22} photons/s/mm^2/mrad^2/0.1%

saturation lengths. The decrease of the FEL output power with the emittance increase is mainly caused by diffraction effects. The corresponding increase of the longitudinal velocity spread gives a small contribution to the efficiency decrease.

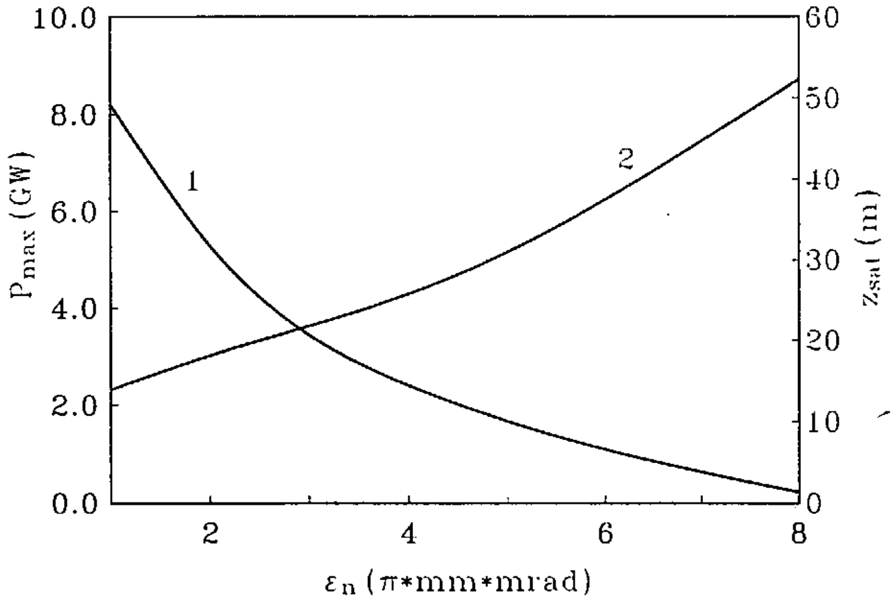

Fig. 2. Dependence of the maximal output power (1) and the saturation length (2) on the value of the normalized emittance. Here $\sigma_E/\mathcal{E} = 0.1$ %. All remaining parameters used for the simulations are listed in Table 1.

3.2 Influence of the energy spread

In Fig.3 we illustrate the influence of the uncorrelated energy spread of the particles in the beam on the FEL amplifier operation. An analysis of these plots indicates that the safety margin for the energy spread is only a factor of 1.5. An increase of the energy spread by a factor of 3 almost destroy the FEL amplifier operation, even if an arbitrary long undulator is assumed.

4 Discussion

In conclusion we should like to make some remarks on the problem of transverse and longitudinal coherence of the output radiation of the SASE FEL. Strictly speaking, the steady-state approximation can not provide quantitative description of this phenomenon. Nevertheless, it is possible to use simple physical considerations, that have been confirmed by a one-dimensional time-dependent model[20]. The longitudinal coherence length is of the order of the cooperation length: $l_c \simeq \lambda l_g/\lambda_w$, where l_g

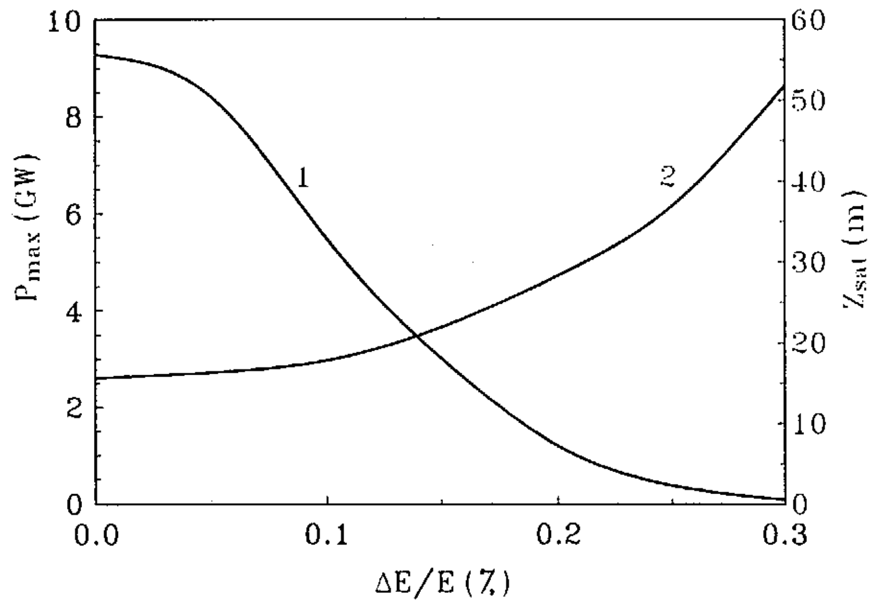

Fig. 3. Dependence of the maximal output power (1) and the saturation length (2) on the value of the energy spread. Here $\epsilon_n = 2\pi$ mm mrad. All remaining parameters used for the simulations are listed in Table 1.

is the gain length. So, if the length of the electron beam σ_z is significantly greater than the cooperation length, there will be temporal dependence of the frequency and amplitude of the output radiation within each pulse. The number of spikes in each pulse is of the order of σ_z/l_c. Also, the spectrum of the output radiation contains many spikes within the bandwidth of the FEL amplifier calculated with steady-state theory[21].

The situation for the transverse coherence of the output signal is somewhat complicated. In the region of parameters of our SASE FEL, the extension of radiation at the gain length is much less than the transverse size of the electron beam, so there is no total transverse coherence of the shot noise at the entrance of the undulator. We can suppose only that the process of amplification from shot noise begins to develop independently in clusters [19]. Simple qualitative consideration can not describe this process and three-dimensional numerical simulations should be performed in the same way as it was done in the one-dimensional model (see refs. [20] and references therein).

Acknowledgement

We thank B.H. Wiik, D. Trines and I. Ivanov for their interest and support in our work. One of the authors (Yu.M.N.) would like to thank the HASYLAB at DESY for their hospitality during her stay in Hamburg and DAAD for the financial support of her work.

References

[1] "A VUV Free Electron Laser at the TESLA Test Facility: Conceptual Design Report", DESY Print TESLA-FEL 95-03, Hamburg, DESY, 1995.

[2] D.A. Edwards, editor, "TESLA Test Facility Linac: Design Report", DESY Print TESLA 95-01, Hamburg, DESY, 1995.

[3] J. Rossbach, Studies on a Free Electron Laser for the TESLA Test Facility, presented at PAC-95.

[4] A.M. Kondratenko and E.L. Saldin, Part. Accel. 10 (1980) 207 and Ya.S. Derbenev, A.M. Kondratenko and E.L. Saldin, Nucl. Instrum. and Methods **193** (1982) 415 and R.Bonifacio, C.Pellegrini, L.Narducci, Opt. Commun. 50 (1984) 373

[5] G.T. Moore, Opt. Commun. **52** (1984) 46

[6] G.T. Moore, Nucl. Instrum. and Methods **A250** (1986) 381

[7] C.-M. Tang and P. Sprangle, IEEE J. Quantum Electron. **QE-21** (1985) 970

[8] E.T. Scharlemann and W.M. Fawley, in Modelling and Simulation of Optoelectronic Systems. SPIE, vol. 642 (1986), p.1, and R.A. Jong, W.M. Fawley and E.T. Scharlemann, in Modelling and Simulation of Optoelectronic Systems. SPIE, vol. 1045 (1989), p.18

[9] T.-M. Tran and J.S. Wurtele, Comp. Phys. Commun. **54** (1989) 263, and P. Jha and J.S. Wurtele, Nucl. Instrum. and Methods, **A331** (1993) 477

[10] J.C. Goldstein, T.F. Wang, B.E. Newnam, and B.D. McVey, Proc. 1987 Particle Accelerators Conf., Washington, DC, USA, p.202

[11] L.H. Yu, S. Krinsky and R.L. Gluckstern, Nucl. Instrum. and Methods **A304** (1991) 516

[12] Y.H. Chin, K.-J. Kim and M. Xie, Nucl. Instrum. and Methods **A318** (1992) 481

[13] E.L. Saldin, E.A. Schneidmiller and M.V. Yurkov, Opt. Commun. **97** (1993) 272, E.L. Saldin, E.A. Schneidmiller and M.V. Yurkov, Opt. Commun. **95** (1993) 141, E.L. Saldin, E.A. Schneidmiller and M.V. Yurkov, Preprint DESY 94-219, Hamburg, DESY, 1994.

[14] Yu.M. Nikitina and J. Pflüger, Two novel undulator schemes with quadrupolar focusing for the VUV-FEL at the Tesla Test Facility, presented at this conference

[15] J. Pflüger and Y.M. Nikitina, Undulator schemes with the focusing properties for the VUV-FEL at the TTF, to be published

[16] B. Faatz, J. Pflüger, P. Pierini, Dependence of the VUV-FEL Performance at the TESLA Test Facility on Magnetic Field Errors, presented at this conference

[17] P.Pierini, W.M.Fawley, Shot Noise Startup of the 6 nm SASE FEL at the TESLA Test Facility, presented at this conference

[18] W. Brefeld, calculations with fitting formulae in accordance with ref. K.J. Kim and M. Xie, Nucl. Instrum. and Methods **A331** (1993) 359

[19] E.L. Saldin, E.A. Schneidmiller and M.V. Yurkov, DESY Print May 1995, TESLA-FEL 95-02, Hamburg, DESY, 1995.

[20] R. Bonifacio et al., Phys. Rev. Lett. **73** (1994) 70, and, R. Bonifacio et al., Nucl. Instrum. and Methods **A341** (1994) 181

[21] K. J. Kim, Phys. Rev. Lett. **57** (1986) 1871

A VUV FREE ELECTRON LASER AT THE TESLA TEST FACILITY AT DESY

J. Rossbach

for the TESLA FEL Study Group[1]

Deutsches Elektronen Synchrotron, D-22603 Hamburg, Germany

Abstract

We present the layout of a Single Pass Free Electron Laser (FEL) to be driven by the TESLA Test Facility (TTF) currently under construction at DESY. The TTF is a test-bed for high-gradient, high efficiency superconducting acceleration sections for a future linear collider. Due to ist unrivaled ability to sustain high beam quality during acceleration, a superconducting rf linac is considered the optimum choice to drive a FEL. We aim at a photon wavelength of λ = 6 nanometers utilizing the TTF after is has been extended to 1 GeV beam energy. Due to lack of mirrors and seed-lasers in this wavelength regime, a single pass FEL and Self-Amplified-Spontaneous-Emission (SASE) is considered. A first test is foreseen at a larger photon wavelength. The overall design as well as both electron and photon beam properties are discussed.

PROOFS:
J. Rossbach
DESY -MPY-
Notkestr. 85
D 22603 Hamburg
Germany
Tel.: +49 40 8998 3617
FAX: +49 40 8994 4305
e-mail: rossbach@desy.de

Tu1 - 2. Presented at the 17th International Free Electron Laser Conference,
August 21 - 25, 1995, New York, NY, USA

[1] The TESLA FEL Study Group:
ASC Samara: E.L. Saldin, E.A. Schneidmiller; **CE Saclay:** A. Mosnier; **DESY:** R. Bacher, W. Brefeld, M. Dohlus, B. Dwersteg, H. Edwards, B. Faatz, J. Feldhaus, K. Flöttmann, A. Gamp, P. Gürtler, K. Hanke, L. M. Kiernan, M. Leenen, T. Limberg, G. Materlik, T. Möller, J. Pflüger, D. Proch, J. Rossbach, J. Schneider, S. Schreiber, M. Seidel, J. Sekutowicz, C. Stolzenburg, K. Tesch, D. Trines, N. Walker, R. Wanzenberg, H. Weise, B.-H. Wiik, S.G. Wipf; **Fermilab Chicago:** E. Colby, T. Nicol; **INFN Milano:** R. Bonifacio, C. Pagani, P. Pierini, L. Serafini; **JINR Dubna:** A. Molodozhentsev, N. Petrov, M.V. Yurkov; **Lawrence Berkeley Laboratory:** W.M. Fawley; **Lawrence Livermore Natl . Lab.:** T. Scharlemann; **Los Alamos Natl. Lab.:** J. Goldstein, R.L. Sheffield; **Max-Born-Institut Berlin:** H. Rottke, W. Sandner, I. Will; **Polish Acad. of Sciences Warschau:** J. Krzywinski; **UCLA Los Angeles:** J. Rosenzweig; **Univ. Hamburg:** C. Kunz, B. Sonntag, H.J. Voß; **Univ. Tomsk, Russia:** Y. Nikitina

1. GENERAL DESCRIPTION

A Free Electron Laser (FEL) in the soft X-ray regime is under study, using the superconducting linac of the TESLA Test Facility (TTF) being under construction at DESY [1,2]. The FEL at the TESLA Test Facility (TTF FEL) is based on the principle of 'Self Amplified Spontaneous Emission' (SASE) [3,4]. Since in the SASE scheme microbunch formation starts from noise, a long undulator is needed to achieve laser action with exponential growth in light output [5]. For the TTF FEL an overall undulator length of 30 m is planned.

Figure 1 shows the overall TTF FEL scheme. Table I compiles main parameters of the TTF FEL. Figure 2 illustrates the spectral brilliance of the TTF FEL in comparison with second and third generation synchrotron radiation sources and the LCLS Free Electron Laser project discussed at SLAC, Stanford, USA [6].

The photon wavelength λ_{ph} of the first harmonic is related to the period length of a planar undulator λ_u by

$$\lambda_{ph} = \frac{\lambda_u}{2\gamma^2}\left(1+\frac{K^2}{2}\right), \qquad (1)$$

where, $\gamma = E/mc^2$ is the relativistic factor of the electrons and $K = e\, B_u\, \lambda_u /2\pi mc$ the 'undulator parameter', e being the elementary charge, m the electron rest mass, c the speed of light, and B_u the peak field in the undulator.

Considerable effort has been made to define an FEL parameter set that is attractive to a wide community of potential users[7]. The physics program for the TTF FEL covers applications ranging from magnetic materials research and various pump-and-probe experiments to photochemistry and X-ray microscopy of biological samples. This program requires a photon wavelength below about 6 nm. Therefore, if state-of-the-art undulator parameters are assumed, e.g. λ_u = 27 mm, K = 1.3, a beam energy of 1 GeV is necessary.

Two beam parameters are essential to reach power saturation within a not too long undulator: A small transverse beam emittance ε_t to provide both small beam diameter and small beam divergence in the undulator, and a small longitudinal beam emittance ε_s to achieve kilo-Ampere instantaneous beam currents at an energy width in the 0.1% range.

The superconducting linear accelerator currently under construction at DESY is an ideal accelerator to drive a SASE FEL. There are two main reasons:

- The perturbation of small emittance beams during the acceleration process is smallest with a superconducting linac at lower frequency. Because the resonator volume and the stored energy are big, the accelerating field is hardly affected by the presence of the electron beam. The variation of the effective accelerating voltage over the bunch length („longitudinal wakefield") is minimum and the tendency of beam induced rf deflections („transverse wakefields") is small.
- A superconducting linac provides a large AC power efficiency and a high duty cycle. The TESLA Test Facility will operate at 1 % duty cycle, orders of magnitude larger than a normal conducting linac would do at the TTF nominal gradient of 15 MV/m. In addition to power efficiency, this is another crucial advantage for potential experiments, because it leaves sufficient time between pulses in the bunch train for data handling.

The most expensive single component of a short wavelength FEL is the accelerator. It is useful to understand that a SASE FEL needs beam parameters similar to those to be realized for a Linear Collider. Thus, the TTF linac can be ideally utilized for driving a

SASE FEL, and there is an extensive common interest in R&D on beam handling and diagnostics. For the discussion of the TESLA Test Facility linac and its relation to the TESLA 500 Linear Collider scheme we refer to the TTF Design Report [1]. It is noted that the TTF FEL is considered a neccessary step to pave the way towards an Ångström FEL which is part of the TESLA500 linear collider scenario.
The TTF design energy is 500 MeV. It has to be upgraded to 1 GeV electron beam energy required for the desired photon wavelength.

2. ELECTRON SOURCE

The transverse coherence condition imposes a tight requirement on the transverse emittance ε_t of the electron beam [8]:

$$\varepsilon_t^n \leq \frac{\gamma \cdot \lambda_{ph}}{4\pi} \qquad (2)$$

ε_t^n is the normalized emittance. For λ_{ph} = 6 nm, γ = 2000, Eq. (2) requires[2] $\varepsilon_t^n < 1\ \pi$ mrad mm. Actually, as is seen from Figure 4, this condition is not very strict, but the saturation length significantly increases if ε_t^n is larger. Thus, we aim at $\varepsilon_t^n = 1\ \pi$ mrad mm for the rms electron emittance of a 1 nC bunch charge from an rf electron gun [9], and we allow for a factor of two emittance dilution during longitudinal beam compression and acceleration up to 1 GeV. According to beam dynamics simulations in both the bunch compressors and the accelerator, this seems to be a conservative assumption.
In spite of very quick acceleration (typically about 30 MV/m in an L-band gun), there is still considerable emittance growth due to space charge forces. By applying solenoid focusing, a bunch rotation in phase space can be performed such, that there is mutual compensation of space charge effects before and after this focusing [10]. First investigations show that, using the described technique, the required emittance should be feasible [11,12,13].

3. LONGITUDINAL BUNCH COMPRESSION AND BEAM DYNAMICS

As mentioned before, a very high instantaneous beam current is needed in the undulator to reach photon power saturation within a reasonable undulator length. For the TTF FEL, this number is 2500 A, corresponding to 50 μm rms bunch length for a 1 nC bunch charge. This value is not attainable directly from the electron gun, because space charge forces would blow up both the transverse beam size and the momentum spread. Thus, the use of magnetic bunch compression is foreseen in order to reduce the rms bunch length from 2 mm in three steps down to 50 μm.

In principle one could consider performing the bunch compression in one step at an energy level, where space charge is not critical any more (> 300 MeV or so). However, even at the comparatively low TTF rf frequency, the cosine-like time dependence of the accelerating field would then impose an intolerable nonlinear correlated energy distribution along the bunch. The proposed solution is to perform compression in three

---

[2] The factor π is only included in the dimensions to indicate that the numerical value of the emittance (in the present case 1) does *not* include π. Following common practice, we nevertheless omit the factor π in formulae describing the beam size etc., i.e. we write $\sigma=\sqrt{\varepsilon_t \cdot \beta}$, instead of, in a mathematically rigorous way, $\sigma = \sqrt{\varepsilon_t / \pi \cdot \beta}$

steps at 22 MeV (2 mm → 0.8 mm), 140 MeV (0.8 mm → 0.25 mm) and 500 MeV (0.25 mm → 0.05 mm) [14].
The uncorrelated energy spread of the beam leaving the gun is around 25 keV, its length 2 mm. The SASE process requires less than 1000 keV energy spread at the undulator. Thus, the initial longitudinal emittance of around 50 mm·keV is already close to the finally tolerable emittance, and the emittance blow up during compression has to be kept small. The final bunch length is basically determined by the ratio of initial to induced energy spread.

Since neither space charge effects nor the nonlinearity of the accelerating voltage nor longitudinal wakefields are completely negligible, computer simulation is required to get a realistic model of beam behaviour along the linac. First results of such an analysis indicate that the aforementioned sequence of compressions seems to be adequate. Figure 3 illustrates an output of such an analysis. It is noted that, due to the comparatively small wakefields in the TESLA modules, the bunch compression scheme does not rely on an exact knowledge of the shape and magnitude of longitudinal wakefields.

4. UNDULATOR

The undulator is the most prominent FEL specific component. It has two functions:

1. It has to provide the sinusoidal field so that the FEL process can take place.
2. In order to keep the beamsize small over the whole undulator length, the undulator has to be supplied with an alternating field gradient provided by a superimposed quadrupole lattice.

The proposed design [15] minimizes technical risks. A planar hybrid undulator is foreseen with period length $\lambda_u = 27$ mm and peak magnetic field $B_u = 0.5$ T, parameters very much like those of existing undulator magnets. The main challenges are the total length of 30 m, the additional quadrupole focusing to be supplied and tight tolerances. First computer simulations with TDA3D on undulator errors indicate that the most critical parameter is the misalignment between electron beam and photon beam (required to be smaller than some 10 μm), while phase fluctuations of the radiation field would become critical only at much larger peak field fluctuations [16].
To simplify production, measurement and installation, 5m long undulator modules are foreseen. This also permits installation of electron and photon beam monitors and correction elements inbetween.

5. FEL PROCESS

Various computer codes have been used to investigate the start-up from noise, and the lethargy, exponential and saturation regimes, respectively, e.g. NUTMEG [17], GINGER [18], FS2R [19], TDA3D [20,21]. There is no essential disagreement between results of all these codes written by different groups and based on different approaches [22]. A critical issue for a SASE FEL is to take into account the time dependence of the input noise and the slippage effects in the theory and in the simulations. The one-dimensional analysis shows that a critical parameter for shot noise analysis is the beam length in units of the "cooperation length" [23]:

$$\ell_c = \frac{\lambda}{4\pi\rho} .$$

For the TTF FEL the cooperation length is 0.26 μm, and the beam length is 50 μm. In this case bunch-to-bunch fluctuations should be a fraction of a gain length and the use of an equivalent input signal analysis should be adequate. This is in agreement with 2D GINGER simulations [24].

A peculiar characteristic of the SASE FEL is the strong spiking both in the temporal and spectral domain of the emitted radiation. It is a consequence of longitudinal subsections inside each electron bunch radiating at statistically independent phases if the start-up is from noise instead of being „seeded" by an external radiation field of high longitudinal coherence (i.e. by a „seed laser"). Calculations with GINGER have confirmed the presence of strong spikes, with a duration of the order of a cooperation length and peak power of about 10 GW [24].

After saturation the FEL behavior is determined by the nonlinear regime of the spikes. The total linewidth (half width half maximum) has been estimated using GINGER at 0.1% [24], which is, due to diffraction effects, even smaller than the FEL parameter, ρ=0.2%, which is the expected value from the 1D time dependent model.

As seeding at 6 nm is impossible due to lack of lasers, schemes generating harmonic content of the longitudinal electron density modulation at (roughly) the 40th harmonic of a conventional laser could be considered (multiple stage harmonic generation [25]). Further studies on these schemes are desirable, but they are presently not proposed for the TTF FEL, because the TTF FEL aims at establishing the SASE mechanism for short wavelengths in order to prepare for an Ångstrøm FEL, on which the multiple stage harmonic generation scheme is even more unlikely to be applicable.

Since, in view of the present state of the art, to achieve the desired transverse electron beam emittance seems to be possible but by far not trivial, the dependence of radiation properties on beam emittance has been studied. Figure 4 shows the emitted intensity as a function of ε_t^n.

Figure 5 shows the photon flux emitted by the TTF FEL without field errors taken into account.

TTF FEL PHASE 1

In order to learn as quick as possible, it is foreseen to perform a first SASE FEL test just after the TESLA Test Facility has been commissioned. This will be in the electron beam energy range between 300 and 500 MeV. Using two or three of the final undulator modules, the resonant photon wavelength will be much larger. Therefore, beam requirements can be relaxed: larger transverse emittance and longer bunch length will be tolerable. The main objectives of this phase are observation of startup from noise and exponential regime, commissioning of all but the final bunch compressors and beam diagnostics. No operation for users is planned during this phase 1 operation.

REFERENCES

[1] D. A. Edwards (ed.): TESLA Test Facility Linac - Design Report, DESY Print TESLA 95-01 (1995)

[2] A VUV Free Electron Laser at the TESLA Test Facility at DESY, Conceptual Design Report, DESY Print TESLA-FEL 95-03 (1995)

[3] A. M. Kondratenko, E.L. Saldin: Part. Accelerators Vol.10, pp 207-216 (1980)

[4] R. Bonifacio, C. Pellegrini, I.M. Narducci: Opt. Commun. **50** (1984) 373.

[5] P. Pierini, W.M. Fawley: Shot Noise Startup of the 6 nm SASE FEL at the TESLA Test Facility, this conference

[6] H. Winick, et al.: Nucl. Instr. Meth. A347, pp 199-205 (1994)

[7] Contributions to the TTF FEL scientific case were made by:
DESY: J. Feldhaus, P. Gürtler, L.M. Kiernan, G. Materlik,, T. Möller, J. Schneider, **FHI Berlin:** U. Becker, A. Bradshaw, P. Hoffmann, FU Berlin: T. Leisner, E. Rühl, N. Schwentner, L . Wöste; **Helsinki Univ. of Technology:** T. Åberg; **KFA Jülich:** W. Eberhard, G.Ganteför, J.E. Rubensson; **Lab. de Photophys. Moléculaire Paris:** G. Comtet, G. Dujardin, L.Hellner; **LNLS Campinas:** R. DeCastro; **Max-Planck-Inst. f. Biophys. Chemie Göttingen:** T. M. Jovin; **Max-Planck-Inst. f. Mikrostrukturphys. Halle:** C. M. Schneider; **Max-Planck-Inst. f. Strömungsforschung Göttingen:** F. Federmann; **Polish Acad. of Science, Warsaw:** K. Rzazewski; **TU Berlin:** P. Zimmermann; **TU München:** P. Feulner, D. Menzel, W. Wurth; **Univ. Bielefeld:** N: Böwering, D. Feldmann; **Univ. Birmingham:** R. E. Palmer; **Univ. Bochum:** K. Al-Shamery, H. J. Freund, W.Greinert; **Univ. Düsseldorf:** E. Kisker; **Univ. Essen:** C. Westphal, H. Zacharias; **Univ. Frankfurt:** H. Schmidt-Böcking, L. Spielberger; **Univ. Freiburg:** W. Kamke; **Univ. Göttingen:** G. Schmahl; **Univ. Hamburg:** C. Kunz, B. Sonntag, H.J. Voß; **Univ. Kiel:** L. Kipp, M.Skibowski; **Univ. Mainz:** H. Backe; **Univ. München:** K. Müller-Dethlefs; **Univ. Rostock:** K. H. Meiwes-Broer; **Univ. Würzburg:** H.-P.Steinrück; **Uppsala Univ.:** M. Martensson

[8] see e.g. W.B. Colson, C. Pellegrini, A. Renieri (eds.): Laser Handbook Vol. 6, North Holland (1990)

[9] J. Fraser, R. Sheffield: Nucl. Instr. Meth. A 250 (1986) 71

[10] B. Carlsten: Nucl. Instr. Meth A 285 (1989) 313

[11] J. Rosenzweig, E. Colby: Charge and Wavelength Scaling of the RF Photoinjectors: A Design Tool, Proc. 1995 Part. Acc. Conf., Dallas (1995)

[12] J.C. Gallardo, H. Kirk, T. Meyerer: A Comparison of L-Band and C-Band rf guns as Sources for Inline-Injection Systems, Proc. 1995 Part. Acc.Conf., Dallas (1995)

[13] K. Flöttmann, et al.: private communication

[14] T. Limberg, et al.: The Bunch Compression System at the TESLA Test Facility FEL, this conference

[15] YU.M. Nikitina, J. Pflüger: Two novel undulator schemes with quadrupolar focusing for the VUV-FEL at the TESLA Test Facility, this conference

[16] B. Faatz, J. Pflüger, P. Pierini: Dependence of the VUV-FEL Performance at the TESLA Test Facility on Magnetic Field Errors, this conference

[17] E.T. Scharlemann, W.M. Fawley, SPIE, Vol. 642, 1 (1986)

[18] R.A. Jong, et al.: SPIE, Vol. 1045, 18 (1989)

[19] E.L. Saldin, et al.: DESY Report 94-219 (1994)

[20] T.-M. Tran, J.S. Wurtele: Comput. Phys. Commun. 54 (1989) 263

[21] P. Jha, J.S. Wurtele: Nucl. Instr. Meth. A331 (1993) 447

[22] W. Brefeld, et al., Parameter Study of the VUV FEL at the TESLA Test Facility, this conference

[23] R.Bonifacio, et al.: Phys. Rev. Lett., 73 (1994), 70

[24] P.Pierini, W.M. Fawley: Shot Noise Startup of the 6 nm SASE FEL at the TESLA Test Facility, this conference

[25] L. Serafini, M. Ferrario, C. Pagani, A. Peretti: SHOK: Sub-Harmonic High-Gain Optical Klystron, INFN/TC-90/11 (1990)

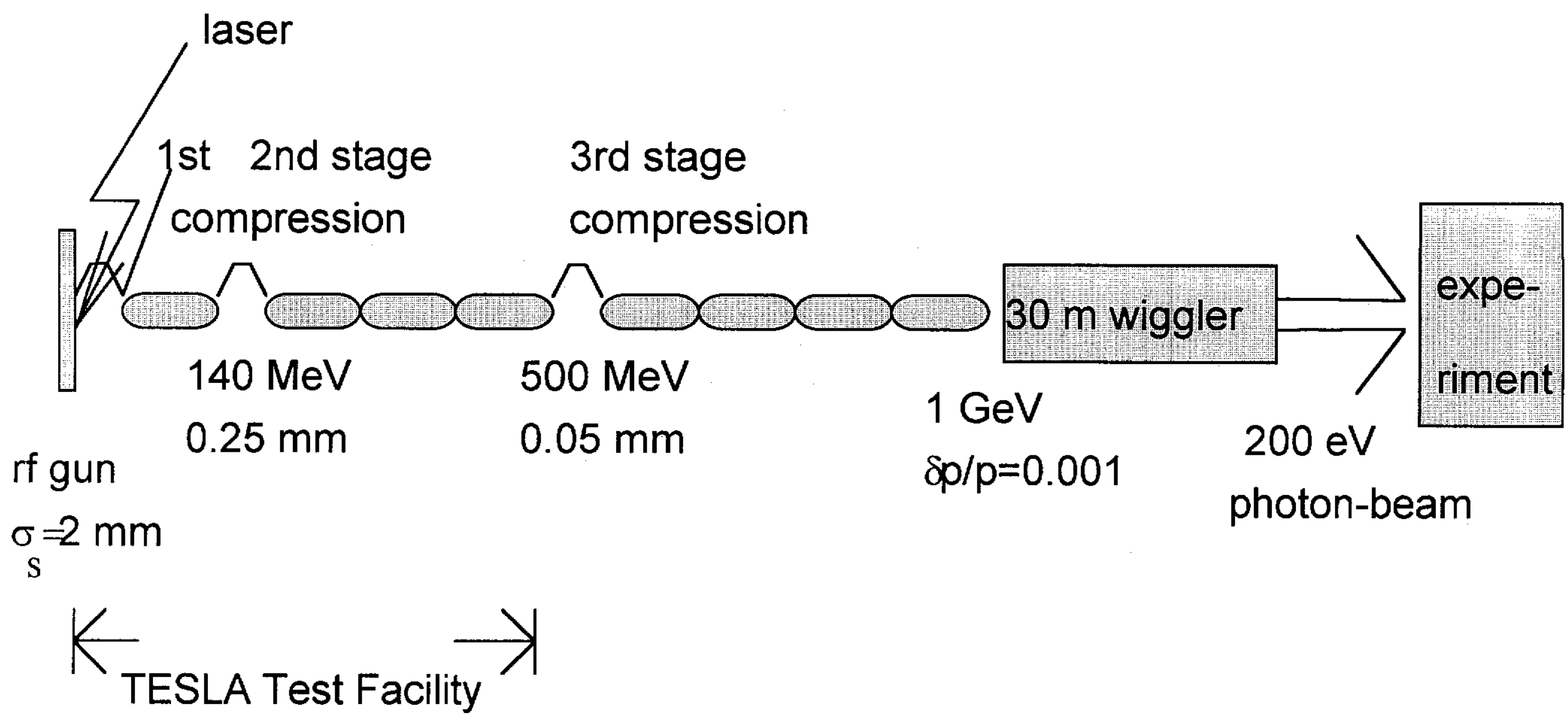

Figure 1: Schematic layout of the TTF FEL based on the TESLA Test Facility (TTF). Four additional TESLA accelerator modules bring the energy up to GeV. The bunch length is reduced from 2 mm to 50 mm within three steps of bunch compression. The SASE FEL process requires an undulator of 25 n effective length. The over-all length of the facility is some 200 meters.

VARIABLE	UNITS	VALUE
beam energy	GeV	1.000
l(radiation wavelength)	nm	6.4 (193 eV)
l_u (undulator period)	mm	27.3
undulator gap	mm	12
B (undulator peak field)	T	0.497
effective undulator length (excluding drift spaces between modules)	m	25
beam optics β function	m	3
rms beam size	mm	0.05
ε^n (normalized emittance) in the undulator	π mrad mm	2.0
peak electron current	A	2490
number of electrons per Gaussian bunch		6.24E+9
number of photons per Gaussian bunch		4E+13
peak electron beam power	GW	2490
rms energy spread σ_γ/γ	10^{-3}	1.00
rms bunch length σ_s	µm	50.
L_g (power gain length)	m	1.00
L_s (saturation length)	m	< 25
P_{sat} (saturated power)	GW	3
average brilliance [photons/s/mm^2/mr/0.1%]		up to 6E+21
bunch train length	µsec	800
number of bunches per train		up to 7200
repetition rate	Hz	10

Table I: Main parameters of the TESLA Test Facility FEL (TTF FEL). The insertion device is assumed to be a planar hybrid undulator. These values should be used as a guideline only since the optimization has not yet been finished and experimental experience has to be gained in this wavelength regime.

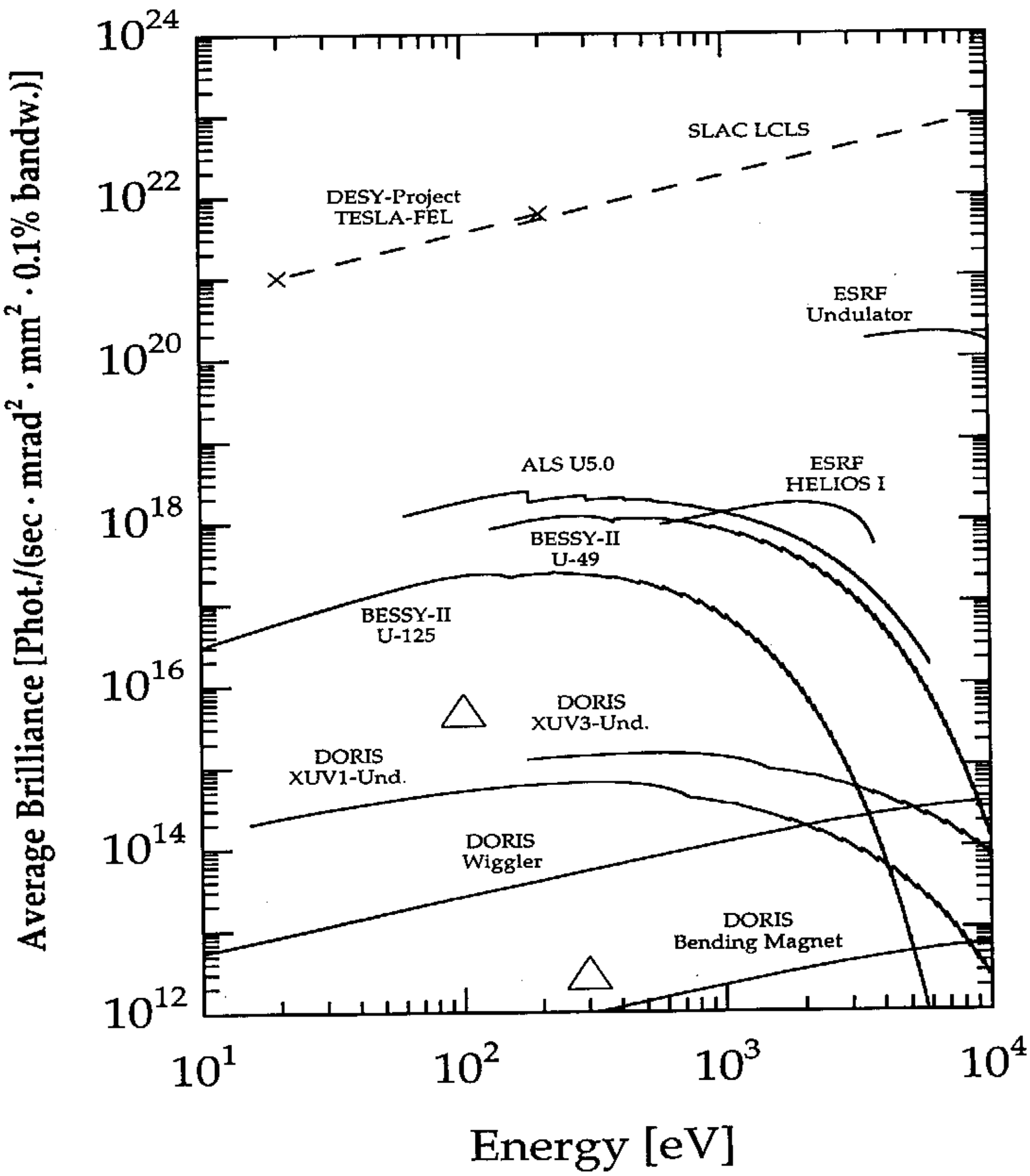

Figure 2: Spectral brilliance of the TTF FEL in comparison with second and third generation synchrotron radiation sources and the LCLS Free Electron Laser project discussed at SLAC, Stanford, USA[5]. The open triangles represent values achieved with plasma lasers under the optimistic assumption that they can fire once a second.

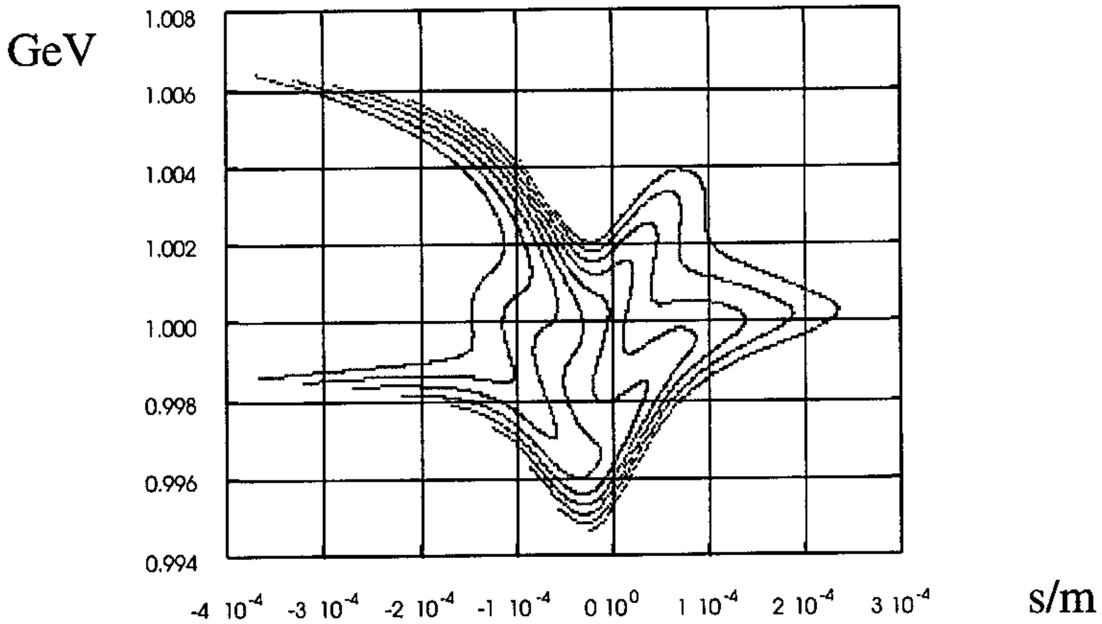

Figure 3: Longitudinal phase space (GeV-m)

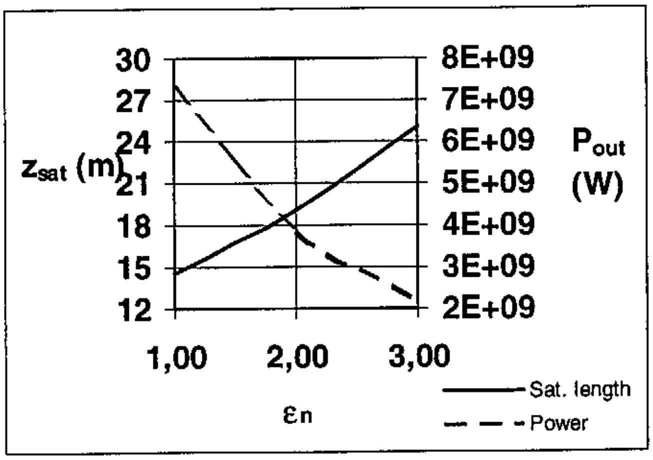

Figure 4: Emitted intensity and saturation length at the peak gain as a function of the normalized electron beam emittance, for the nominal energy spread of 0.1%.

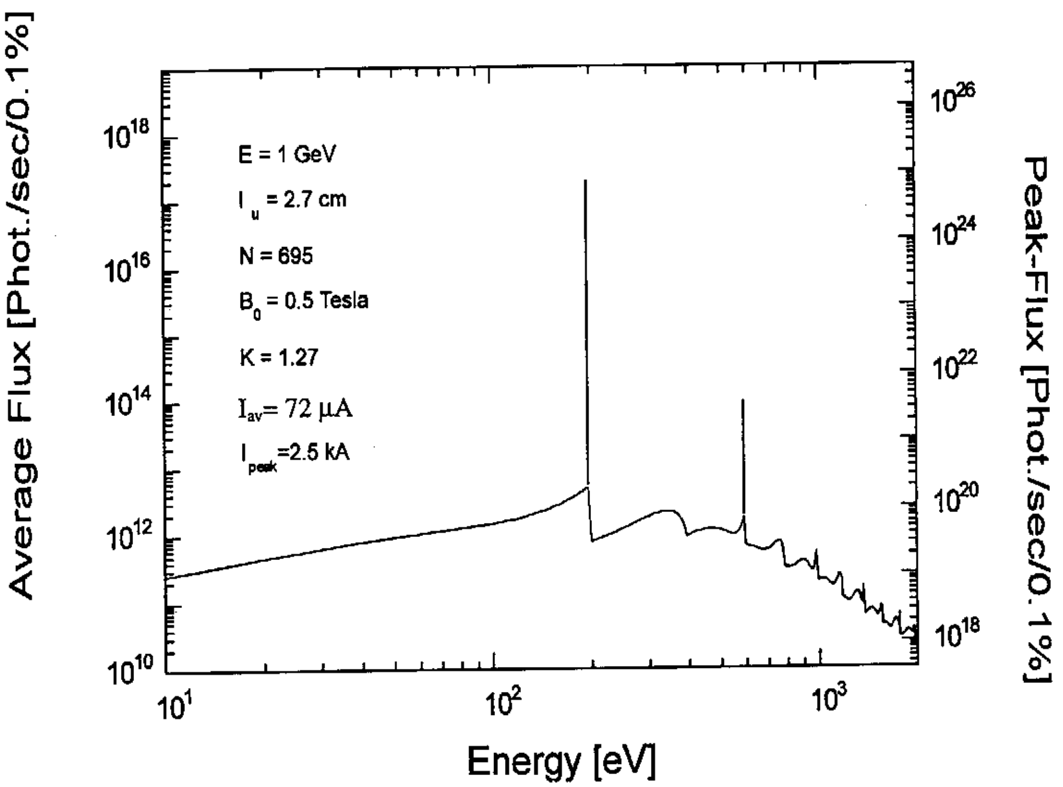

Figure 5: Expected photon flux emitted by the TTF SASE FEL. The two peaks correspond to the FEL emission at the fundamental and 3rd harmonic. The lower curve is the spontaneous emission in the undulator.

Shot Noise Startup of the 6 nm SASE FEL at the TESLA Test Facility *

P. Pierini [a] and W.M. Fawley [b,1]

[a] *INFN Sezione di Milano, Laboratorio LASA, Via F.Cervi, 201, I-20090 Segrate (MI), Italy*

[b] *Lawrence Berlekey Laboratory, University of California, 1 Cyclotron Rd., Berkeley, CA, USA 94720*

We present here the results of an extensive simulation activity for the TESLA SASE FEL. We have used the program GINGER to determine the FEL saturation length and the power fluctuations from shot to shot. The spectral properties of the output power and the correlation functions are investigated and compared with available theoretical models.

PROOFS:

Paolo Pierini

INFN Milano - LASA

Via Cervi, 201

20090 Segrate (MI)

Italy

tel.: +39 2 2392560

FAX: +39 2 2392543

e-mail: pierini@mi.infn.it

* Th3-64. Presented at the 17th International Free Electron Laser Conference, August 21-25, 1995, New York, NY, USA

[1] This work was supported by the Director, Office of High Energy and Nuclear Physics, U.S. Department of Energy, under Contract No. DE-AC03-76SF00098.

Preprint submitted to Elsevier Preprint *10 August 1995*

1 Introduction

Currently, DESY[1] and collaborators are designing a VUV Free Electron Laser (FEL) operating in Self Amplified Spontaneous Emission (SASE) mode. One of the merits of the SASE scheme is that it does not require any input signal from a master oscillator, since the spontaneous radiation emitted by a sufficiently intense electron beam entering in the undulator drives the high gain collective instability[2,3]. A proper study of the shot noise startup, the correct saturation length and its fluctuations requires that the time dependence of the initial shot noise of the electron phases and slippage effects must be taken into account, both in the theory and in the numerical modeling.

The 1D analysis[4] of a SASE-mode FEL shows that depending on the relative length of the electron pulse with respect to the "cooperation length", defined as $\ell_{\rm coop} = \lambda/(4\pi\rho)$ where ρ is the dimensionless FEL parameter[2], the system can operate in very different dynamical regimes. In the long bunch case, when the beam is much longer than the cooperation length, the time structure of the output radiation beam is dominated by the onset of superradiant spiking, seeded by the shot noise nonuniformities. In the short bunch case by contrast, the output pulse consists of a single, clean superradiant pulse, which will exhibit strong shot-to-shot fluctuations.

Previously (see Refs.[1,5]), the beam and undulator parameters for the TESLA FEL have been extensively studied and optimized (see Table 1) in the framework of the steady state, monochromatic theory and simulation, where slippage effects are neglected. In this approximation, the SASE device is modeled as an amplifier seeded with the spontaneous radiation emitted in the first gain length of the undulator.

In this paper we investigate the time structure and spectral characteristics of the emitted pulses from the TESLA FEL, seeking an estimate of the emitted bandwidth and the amplitude of shot-to-shot fluctuations in output power and saturation length.

2 TESLA FEL modeling

Our analysis of the shot noise startup of the TESLA FEL employs the 2D, time-dependent simulation code GINGER[6], which models the interaction of the 3D motion of the beam electrons with an axisymmetric, polychromatic radiation field. The electron and radiation pulses are allowed to travel the wiggler with different velocities. In addition to a time-dependent radiation field, GINGER can also include time-dependent electron beam parameters such as arbitrary current or energy distributions. SASE startup from shot noise is modeled by adding random fluctuations to the macroparticle longitudinal and transverse coordinates[7].

The simulations described here have been performed with a 6D gaussian distribution in the electron phase space. A series of runs has been performed with different random number seeds to assess the influence of shot-to-shot fluctuations over the relevant quantities of the FEL. The beam parameters were set to the nominal values listed in Table 1.

2.1 Spectrum, bandwidth and superradiant spiking

From the analytical theory of a SASE-mode FEL[3,4], it is possible to evaluate the evolution of the half-width of the power spectrum and the decay time of the field autocorrelation function along the wiggler:

$$\left.\frac{\Delta\omega}{\omega}\right|_{\mathrm{HWHM}} = 6\sqrt{\frac{\ln 2}{\sqrt{3}}}\frac{\rho}{z/\ell_{\mathrm{gain}}} \tag{1}$$

$$\tau_{1/2} = \frac{2}{3}\frac{\ell_{\mathrm{coop}}}{c}\sqrt{3\ln 2}\sqrt{\frac{z}{\ell_{\mathrm{gain}}}} \tag{2}$$

where $\tau_{1/2}$ is the time required by the electric field autocorrelation function to decay to 0.5 and $\ell_{\mathrm{gain}} = \lambda_w/(4\pi\rho)$ is the gain length. These relations neglect 2D effects such as diffraction and emittance, and also presume a cold beam with with no energy spread. Thus, eq. (1) represents an upper limit for the FEL bandwidth, since inclusion of energy spread and 2D effects will decrease ρ and the narrow the gain bandwidth.

In Fig. 1 we compare the bandwidth and the autocorrelation time computed from a series of 10 GINGER simulation with expressions (1)-(2). The error bars on the simulation points denote the magnitude of the rms fluctuations around the average value computed from the runs. As was found in previous GINGER simulations of a 4 nm FEL operating in SASE mode[7], $\tau_{1/2}$ grows with the $\sqrt{z}$ dependence predicted in eq. (2) with an absolute magnitude $\sim$ 30% greater due to 2D effects. Likewise, we see that the system experiences a systematic bandwidth narrowing with respect to the 1D theory, due to diffraction. For the parameters used in this simulation the initial Rayleigh range ($z_r = \pi\sigma^2/\lambda$) of the radiation beam is 1.87 m, whereas the 1D gain length is 1.3 m. From the GINGER simulations, the predicted TESLA FEL bandwidth (HWHM) for the power spectrum is approximately 0.1%, which is $\sim$ 60% that of the "natural" FEL bandwidth given approximately by ρ, again due to diffraction effects.

The temporal structure of the emitted pulse (see Fig.2) shows the presence of superradiant spikes seeded from the shot noise on the input electron beam. For the TESLA FEL parameters, the beam length is much larger than the cooperation length and the resulting temporal structure is dominated by sharp superradiant spikes, some of which reach more than 10 GW peak power. This spiking behavior also dominates the spectrum of the emitted radiation in Fig. 2, where the wavelength is resolved in bins of width 2.73×10^{-4} nm. As different shot noise realizations generally lead to different spike positions and relative power, Fig. 2 should be considered as output from a representative "sample" shot.

The behavior of these superradiant spikes follows accurately the predictions of the 1D SASE theory. In particular, the spikes show an overall width which is related to the cooperation length and travel at the group velocity previously predicted by Ref.[4] to be

$$v_{\rm g} = 3\,\frac{v_{\|}}{2+v_{\|}/c} \tag{3}$$

Eq. (3) clearly suggests that the spike velocity is smaller than the light velocity in free space and that the spikes move forward with respect to the electron bunch at approximately one third of the nominal slippage rate of the radiation. This behavior is clearly confirmed by Figure 3, where the normalized radiation intensity, $\hat{I}(z,t) = I(z,t)/\langle I(z)\rangle$, from a TESLA GINGER run is plotted as a function of the distance along the wiggler (horizontal axis) and of a time measured on a frame moving at the light velocity (vertical axis). In this case, to show the dynamics of a few superradiant spikes, we have modeled a very thin longitudinal slice of the electron beam, only 7 μm long (23 fs), imposing periodic boundary conditions at its edges. It is clearly seen from the figure that the spikes move slower than the light velocity during the exponential growth of the power up to saturation (and hence accumulate a time delay on the coordinate $\tau \propto t - z/c$). Near saturation ($z \approx 20\,$m), nonlinear gain effects become important and the radiation spikes start propagating at c (*i.e.* they begin to move horizontally in Fig. 3).

2.2 Average emitted power and saturation length fluctuations

Ref.[4]'s 1D analysis of the SASE startup also predicted, in the case where the beam length is much greater than the cooperation length, that shot-to-shot fluctuations for output power and saturation length become quite small. In Fig. 4 we show both the behavior of the average laser power (4a) and its relative fluctuations (4b) as functions of distance along the wiggler. As expected, the relative shot-to-shot power fluctuations are greatest in the exponential regime where, for the TESLA FEL parameters, these can reach a value of 15-20%.

Well beyond saturation, the relative fluctuation level drops sharply, indicating that while the necessary saturation length may vary somewhat from shot-to-shot, the saturation power is nearly constant.

3 Conclusions

In this paper we have used the time-dependent, 2D simulation code GINGER to examine the predicted operation of the TESLA SASE-mode FEL. The main characteristics of the emitted radiation, the predicted output FEL bandwidth, the temporal correlation function, and the shot-to-shot power fluctuations are generally in good agreement with the available 1D theory, except that the bandwidth is somewhat narrowed due to diffraction effects. The measured group velocity of the temporal radiation spikes also agrees well with the theory.

4 Acknowledgments

The Authors are grateful to the Members of the Study Group of the TESLA FEL collaboration for the many useful discussions.

References

[1] "A VUV Free Electron Laser at the TESLA Test Facility at DESY: Conceptual Design Report", DESY PRINT, June 1995, TESLA-FEL 95-03;

[2] R. Bonifacio, C. Pellegrini, L. Narducci, *Opt. Commun.*, **50**, (1984), 373;

[3] K.J. Kim, *Phys. Rev. Lett.*, **57**, (1986), 1871;

[4] R. Bonifacio, L. De Salvo, P. Pierini, N. Piovella and C. Pellegrini, *Phys. Rev. Lett.*, **73**, (1994), 70;

[5] W. Brefeld, B. Faatz, Yu.M. Nikitina, J. Pflüger, P. Pierini, J. Rossbach, E.L. Saldin, E.A. Schneidmiller, M.V. Yurkov, "Parameter Study of the VUV FEL at the TESLA Test Facility", these Proceedings.

[6] R.A. Jong, W.M. Fawley, E.T. Scharlemann, "Modeling and Simulation of Laser Systems", **SPIE 1045**, (1989), 18;

[7] W.M. Fawley, A.M. Sessler, E.T. Scharlemann, in *Proceedings of the 1993 Particle Accelerator Conference*, Washington, D.C., USA, May 17-20, 1993.

Table 1
Main parameters of the TESLA FEL[1,5].

Total bunch charge	1 nC
Peak current	2.5 kA
Beam energy	1 GeV
rms normalized emittance	2π mm mrad
rms energy spread	0.1%
rms beam length	50 μm (166 fs)
Undulator wavelength λ_w	27.3 mm
Undulator strength a_w	0.896
FEL parameter ρ	1.67×10^{-3}
1D gain length ℓ_{gain}	1.3 m
1D cooperation length ℓ_{coop}	0.3 μm (1.02 fs)

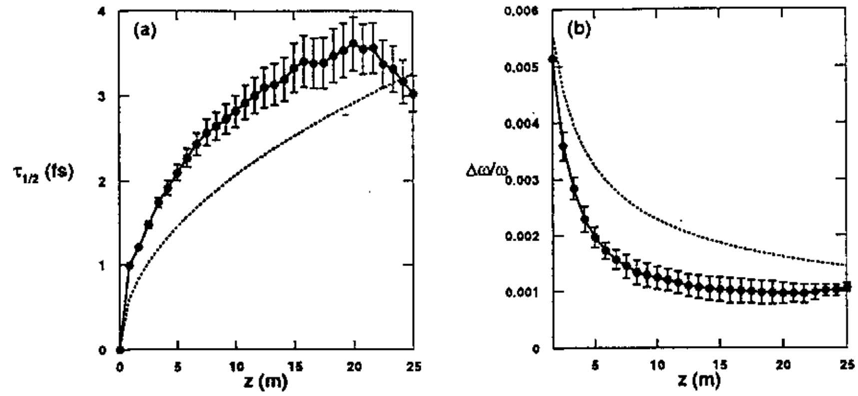

Fig. 1. HWHM of the autocorrelation function (a) and power spectrum halfwidth (b) computed from a series of 2D GINGER runs (solid line and dots with error bars) and the predictions of the 1D analysis (dashed line).

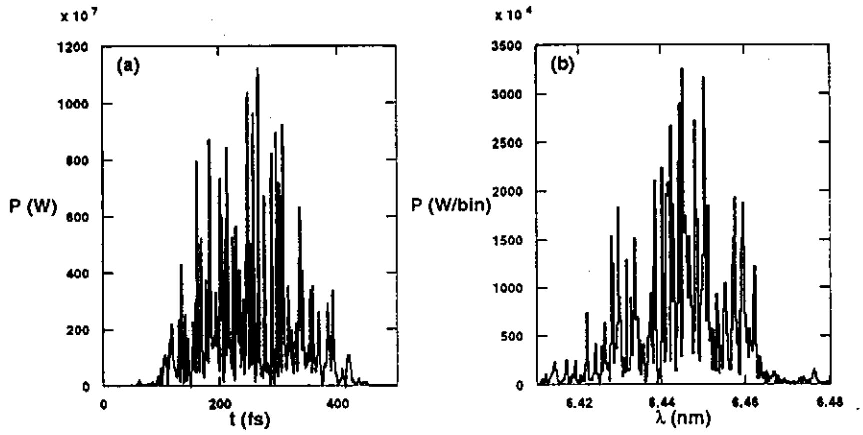

Fig. 2. Predicted temporal structure (a) and spectrum (b) of a typical output radiation pulse of the TESLA SASE FEL.

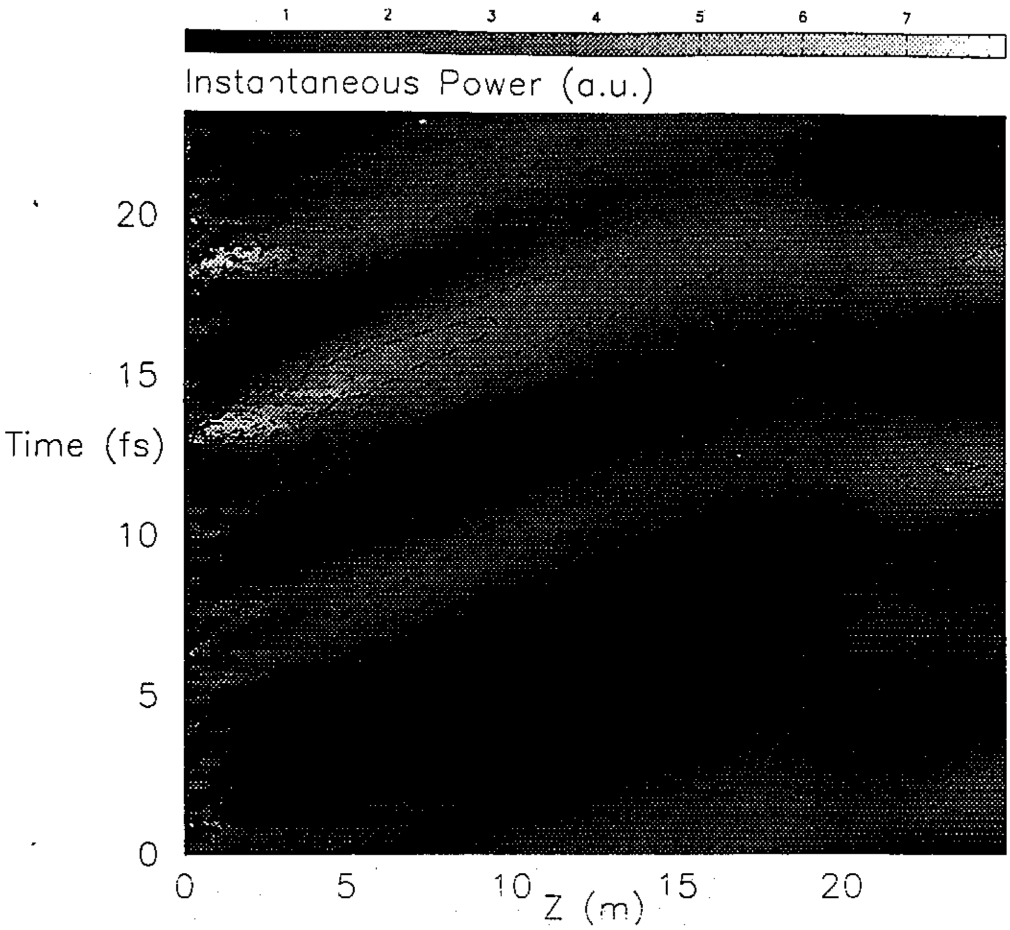

Fig. 3. Plot of the normalized radiation intensity as a function of the wiggler length (horizontal axis) and of the time along a reference frame moving at the light velocity, c (vertical axis). For a description of the figure, please refer to the text.

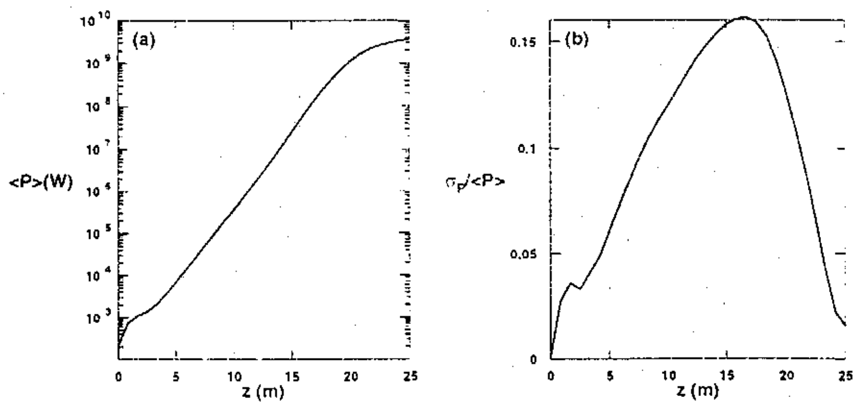

Fig. 4. Evolution of the average emitted power along the wiggler (a) and of the relative power fluctuations along the wiggler (b).